Circadian autophagy drives iTRF-mediated longevity

https://doi.org/10.1038/s41586-021-03934-0

Received: 9 June 2020

Accepted: 19 August 2021

Published online: 29 September 2021

Check for updates

Matt Ulgherait[1], Adil M. Midoun[2], Scarlet J. Park[3,4], Jared A. Gatto[1], Samantha J. Tener[1], Julia Siewert[1], Naomi Klickstein[5], Julie C. Canman[6], William W. Ja[3,4] & Mimi Shirasu-Hiza[1]✉

Time-restricted feeding (TRF) has recently gained interest as a potential anti-ageing treatment for organisms from *Drosophila* to humans[1–5]. TRF restricts food intake to specific hours of the day. Because TRF controls the timing of feeding, rather than nutrient or caloric content, TRF has been hypothesized to depend on circadian-regulated functions; the underlying molecular mechanisms of its effects remain unclear. Here, to exploit the genetic tools and well-characterized ageing markers of *Drosophila*, we developed an intermittent TRF (iTRF) dietary regimen that robustly extended fly lifespan and delayed the onset of ageing markers in the muscles and gut. We found that iTRF enhanced circadian-regulated transcription and that iTRF-mediated lifespan extension required both circadian regulation and autophagy, a conserved longevity pathway. Night-specific induction of autophagy was both necessary and sufficient to extend lifespan on an ad libitum diet and also prevented further iTRF-mediated lifespan extension. By contrast, day-specific induction of autophagy did not extend lifespan. Thus, these results identify circadian-regulated autophagy as a critical contributor to iTRF-mediated health benefits in *Drosophila*. Because both circadian regulation and autophagy are highly conserved processes in human ageing, this work highlights the possibility that behavioural or pharmaceutical interventions that stimulate circadian-regulated autophagy might provide people with similar health benefits, such as delayed ageing and lifespan extension.

iTRF extends *Drosophila* lifespan

We tested four TRF schedules, biased to night-time fasting, for lifespan extension (Fig. 1a, Extended Data Fig. 1a). The control diet provided 24-h access to food (ad libitum). The standard TRF schedule (12-h access to food during lights on, 12-h fasting during lights off) did not extend lifespan relative to the control diet unless limited to adult days 10–40 (days post-eclosion); TRF-mediated lifespan extension was modest and inconsistent from trial to trial[2,6] (Extended Data Fig. 1b, c). By contrast, 24-h fasting (followed by 1–2 days of ad libitum feeding)[6] shortened lifespan, as shown previously[6] (Extended Data Fig. 1d). By trial and error, we identified an intermediate feeding schedule that robustly extended lifespan (Fig. 1a). Flies fasted for 20 h every other day, starting at mid-morning (6 h after lights on or Zeitgeber time 6 (ZT6)), with a recovery day of an ad libitum diet between fast days. Although maintaining this diet through old age did not extend lifespan, maintaining this diet for a 30-day window from 10 to 40 days old resulted in consistent, significant lifespan extension (Fig. 1b, Extended Data Fig. 1e, f). Shorter 10-day windows of this diet at different ages (days 10–20, 20–30 or 30–40) extended lifespan incrementally (Extended Data Fig. 2a–e); by contrast, a 10-day window of this diet with older flies (days 40–50) did not extend lifespan (Extended Data Fig. 2f, g). Relative to animals on ad libitum diets, animals on this diet from days 10 to 40 had a mean lifespan increase of more than 18% (female flies) and 13% (male flies); hereafter, our experiments focused on female flies. We term this lifespan-extending dietary regimen iTRF.

iTRF differs from dietary restriction

We first tested whether iTRF causes caloric restriction, or decreased food intake, which is known to extend lifespan[1,7]. To test food intake, we measured the feeding rates of flies on ad libitum and iTRF diets over three cycles of fasting and refeeding via the capillary feeder (CaFe) assay[8,9]. Flies on an iTRF diet exhibited compensatory feeding during the recovery period (Extended Data Fig. 2h), resulting in slightly increased average food consumption over 48 h (fast day plus feed day), relative to control animals on an ad libitum diet (Fig. 1c). Thus, iTRF does not extend lifespan by limiting nutrient intake.

In flies, two established lifespan-extending manipulations are dietary protein restriction (DR) and inhibition of insulin-like signalling[10]. To test whether iTRF acts via DR to extend lifespan, we titrated protein concentration with either ad libitum or iTRF regimens (Fig. 1d, Extended Data Fig. 2i). If iTRF acts solely via DR, we would not expect iTRF and DR to have additive effects. We found that iTRF and DR can act additively. Thus, iTRF-mediated lifespan extension can function independently of DR-mediated longevity. Similarly, inhibition of insulin-like signalling via

[1]Department of Genetics and Development, Columbia University Vagelos College of Physicians and Surgeons, New York, NY, USA. [2]Department of Biology, École Normale Supérieure, PSL Research University, Paris, France. [3]Skaggs Graduate School, The Scripps Research Institute, Jupiter, FL, USA. [4]Department of Neuroscience, The Scripps Research Institute, Jupiter, FL, USA. [5]Department of Biological Sciences, Columbia University, New York, NY, USA. [6]Department of Pathology and Cell Biology, Columbia University Vagelos College of Physicians and Surgeons, New York, NY, USA. ✉e-mail: ms4095@cumc.columbia.edu

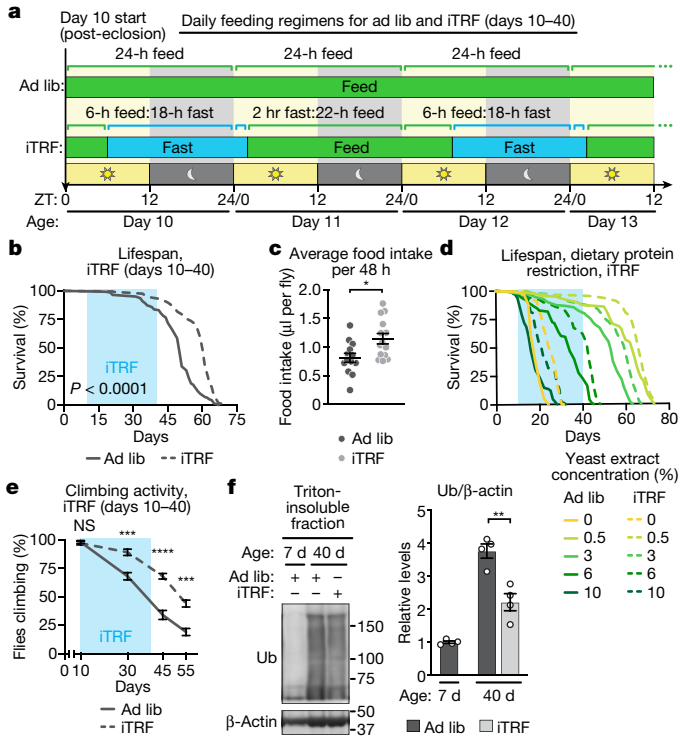

Fig. 1 | iTRF extends lifespan and healthspan without dietary restriction. **a**, Schematic of ad libitum (ad lib) and iTRF diets. **b**, Relative to ad libitum (solid line, $n = 142$), iTRF (dashed line, $n = 205$) extended lifespan ($P < 0.0001$). **c**, Relative to ad libitum (dark grey dots, $n = 13$), flies on iTRF have increased average food intake (light grey dots, $n = 14$). **d**, iTRF and DR additively extended lifespan ($n > 98$ for each diet). **e**, **f**, iTRF decreased age-related declines in climbing activity ($n = 10$ vials of 10 flies per genotype per condition per time point) (**e**) and increased protein aggregation ($n = 4$ biological replicates of 30 flies per genotype per condition per time point) (**f**). Ub, ubiquitin. In **b**, **d**, **e**, the light blue boxes on the graphs indicate the duration of iTRF. See Methods and Supplementary Information for trials, statistics and source data; NS = $P > 0.05$, $^{*}P < 0.05$, $^{**}P < 0.01$, $^{***}P < 0.001$ and $^{****}P < 0.0001$; n refers the number of flies unless otherwise specified; P values were obtained by unpaired, two-tailed t-test (**c**, **f**), ANOVA followed by Tukey's post-hoc test (**e**), and log-rank analysis (**b**, **d**). The centre values are the averages and the error bars indicate s.e.m.

ablation of most insulin-producing cells allowed typical iTRF-mediated lifespan extension with similar magnitude to controls (Extended Data Fig. 2j). Together, these results suggest that iTRF-mediated lifespan extension is distinct from lifespan extension due to DR or inhibition of insulin-like signalling.

iTRF extends healthspan

To assess the anti-ageing effects of iTRF, we assayed known age-related changes in muscle/neuronal function, protein aggregation and intestinal function. First, to assess overall muscle/neuronal function, we assayed climbing ability. Flies on iTRF exhibited less age-related decline in climbing ability relative to flies on an ad libitum diet (Fig. 1e). Second, to measure conserved markers of age-related protein aggregation, we extracted Triton-insoluble fractions from whole-fly extracts of flies on iTRF and ad libitum diets both pre-iTRF and post-iTRF intervention (7 and 40 days old) followed by western blot analysis for ubiquitin (Fig. 1f) and the *Drosophila* orthologue of p62/SQSTM1/ref(2)P (hereafter referred to as p62) (Extended Data Fig. 3a, b). For both markers, flies on iTRF had decreased levels in the insoluble fraction relative to control (ad libitum) flies, demonstrating less ageing-related protein aggregation. Third, we directly measured protein aggregation in muscle using anti-polyubiquitin and anti-p62 antibodies with confocal immunofluorescence microscopy. Again, relative to controls on an ad libitum diet, iTRF significantly decreased the number and area of polyubiquitin and p62 aggregates in the flight muscle of aged flies (Extended Data Fig. 3c–e). Fourth, because decreased intestinal function is another conserved marker of ageing, we measured ageing-related intestinal stem cell over-proliferation, intestinal integrity and intestinal microbial load. iTRF decreased these intestinal ageing markers relative to controls on an ad libitum diet (Extended Data Fig. 3f–h). Finally, because diet affects intestinal microorganisms, which impact ageing, we tested whether iTRF-mediated lifespan extension depends on fly-associated microorganisms. Treatment with antibiotics during both fasting and feeding phases depleted associated microorganisms to nearly non-detectable levels (Extended Data Fig. 3h); iTRF caused the same lifespan extension in antibiotic-treated flies as vehicle controls, suggesting that iTRF-mediated lifespan extension does not depend on fly-associated microorganisms (Extended Data Fig. 3i, j). Together, these results demonstrate that iTRF decreased multiple ageing parameters relative to controls on an ad libitum diet and suggest that iTRF extends lifespan by increasing healthspan and delaying ageing.

iTRF requires an intact circadian clock

Because iTRF does not alter dietary composition but controls the timing of feeding, we examined the role of circadian clock components, which regulate the timing of physiological functions. Circadian clock components are highly conserved among animals[11,12] and regulate 24-h oscillations in transcription, which underlie 24-h oscillations in physiology and behaviour[13,14]. The core circadian clock components form a transcriptional negative-feedback loop[15]: in *Drosophila*, Clock (Clk) and Cycle (Cyc) proteins activate the transcription of hundreds of genes, including many metabolic genes[3,7], and the circadian regulators *period* (*per*) and *timeless* (*tim*), whose gene products inhibit the activity of Clk and Cyc (Fig. 2a).

Others have shown that TRF regimens enhance circadian gene expression[1,3,16–20]. To confirm this effect with iTRF, we performed quantitative real-time PCR (qRT–PCR) analysis of animals on ad libitum and iTRF diets every 4 h for 48 h. iTRF broadened the daytime peak of *clock* (*Clk*) expression (Fig. 2b) and increased the amplitude of *per* and *tim* gene expression, specifically during the night/fasting phase (Fig. 2c, Extended Data Fig. 4a). Thus, similar to other TRF regimens, iTRF enhances circadian gene expression.

To test whether circadian clock components are required for iTRF-mediated lifespan extension, we compared several arrhythmic circadian mutants and their genetic controls on ad libitum and iTRF diets: Clk^{jrk}, cyc^{01}, per^{01} and tim^{01} mutants and mutants with CRISPR-mediated disruption of *per* (per^{CRISPR}) or *tim* (tim^{CRISPR})[21,22] (Fig. 2d, e, Extended Data Fig. 4b, c). While genetic controls exhibited significant lifespan extension on iTRF, circadian mutants did not. As shown previously, per^{01} and cyc^{01} mutants responded normally to DR[23] (Extended Data Fig. 4d, e). Starvation and feeding assays confirmed that, like controls, per^{01} mutants did not die during or after 20-h fast periods and compensated for fast periods with increased feeding[22,23] (Extended Data Fig. 4f, g). Together, our results suggest that iTRF-mediated lifespan extension requires a functional circadian clock.

To test whether iTRF-mediated lifespan extension requires a night-biased fast period, we tested day-biased iTRF, shifted by 12 h (ZT18–ZT14 the following day), with mainly daytime fasting. While night-biased iTRF significantly extended lifespan relative to controls on an ad libitum diet, day-biased iTRF did not (Fig. 2f). per^{01} mutants were unaffected by either iTRF regimen. This result suggests that night-biased fasting is required for iTRF lifespan extension.

To test whether iTRF-mediated healthspan extension is dependent on the circadian clock, we measured climbing ability and ubiquitylated protein accumulation for young and old per^{01} mutants and genetic controls on iTRF or ad libitum diets. While iTRF preserved climbing ability and lowered ubiquitylated protein levels in controls relative to those

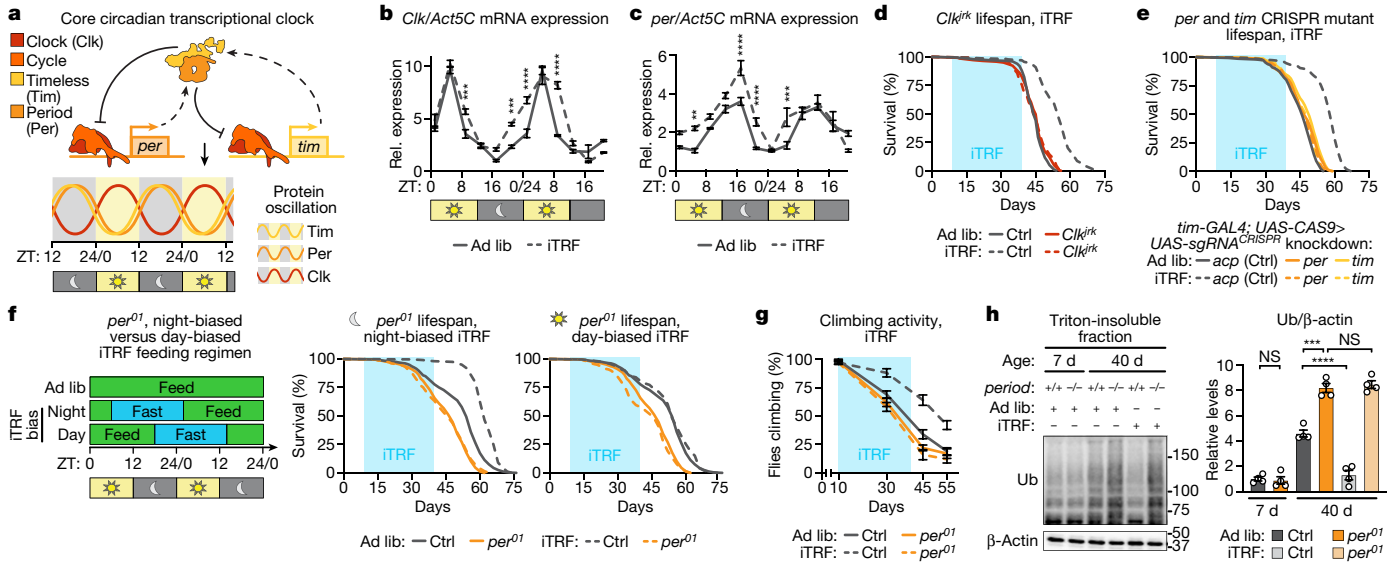

Fig. 2 | Core circadian clock components are required for iTRF-mediated lifespan and healthspan extension. a, Schematic of the core circadian clock. **b**, **c**, Relative to an ad libitum diet (solid line), iTRF (dashed line) enhanced circadian expression of *Clk* (**b**) and *per* (**c**) during fasting ($n = 4$ biological replicates of 30 flies per condition per time point; unmarked is NS). **d**, **e**, Relative to an ad libitum diet (solid lines), iTRF (dashed lines) extended the lifespans of controls (Ctrl; grey; ad libitum $n = 145–199$, iTRF $n = 231–262$) but not Clk^{jrk} mutants (red; ad libitum $n = 143$, iTRF $n = 196$) (**d**), nor tim^{CRISPR} mutants (yellow; ad libitum $n = 228$; iTRF $n = 262$) and per^{CRISPR} mutants (orange; ad libitum $n = 179$, iTRF $n = 192$) (**e**). **f**, In contrast to night-biased iTRF (left graph, dashed grey line; $n = 322$), day-biased iTRF (right graph, dashed grey line; $n = 286$) did not extend lifespan relative to the ad libitum diet (solid grey line; $n = 553$); per^{01} mutants (orange lines) were not affected by night-biased or day-biased iTRF ($n = 209–218$). **g**, **h**, Relative to an ad libitum diet (solid line or dark shade), iTRF (dashed line or light shade) inhibited two ageing markers in controls (grey lines) but not in per^{01} mutants (orange lines): declines in climbing activity ($n = 10$ vials of 10 flies per genotype per condition per time point) (**g**); and increased protein aggregation ($n = 4$ biological replicates of 30 flies per genotype per condition per time point) (**h**). In **d**–**g**, the light blue boxes on the graphs indicate the duration of iTRF. See Methods and Supplementary Information for trials, statistics and source data; NS = $P > 0.05$, $^{**}P < 0.01$, $^{***}P < 0.001$ and $^{****}P < 0.0001$; n refers to the number of flies unless otherwise specified; P values were obtained by ANOVA followed by Tukey's post-hoc test (**b**, **c**, **g**, **h**) and log-rank analysis (**d**–**f**). The centre values are the averages and the error bars indicate s.e.m.).

on ad libitum diets, per^{01} mutants did not respond to iTRF and exhibited ageing-related declines in climbing ability and increased protein aggregation similar to per^{01} mutants on an ad libitum diet (Fig. 2g, h, Extended Data Fig. 4h, i). Thus, iTRF-mediated lifespan and healthspan extension require a functional circadian clock and night-biased fasting.

iTRF requires autophagy components

Because TRF involves fasting, we examined the role of autophagy, a starvation-induced cellular process to recycle macromolecules[24,25] (Fig. 3a). We first used qRT–PCR to test whether two conserved autophagy mediators, Atg1 and Atg8a (the mammalian homologues of ULK1 and LC3, respectively), are circadian-regulated in *Drosophila*. Consistent with other model organisms and cell culture results[26,27], both *atg1* and *atg8a* were circadian-regulated in flies, with night-time expression peaks (Fig. 3b, c, solid lines). Similar to circadian genes, iTRF enhanced night-time expression of *atg1* and *atg8a* in controls (Fig. 3b, c, dashed lines) but not in per^{01} mutants (Extended Data Fig. 5a, b). Thus, expression of two key autophagy genes is circadian-regulated and enhanced by iTRF.

To test whether iTRF induces autophagy, we measured signalling markers of autophagy, autophagic flux and autophagosome/autolysosome formation. We compared genetic controls and per^{01} mutants on iTRF and ad libitum diets, predicting that, if autophagy is a key circadian-regulated function in iTRF, per^{01} mutants would not respond. We first examined two signalling markers associated with autophagy induction: increased AMPK phosphorylation and decreased S6K phosphorylation[28]. Consistent with iTRF-enhanced circadian-regulated autophagy, iTRF fasting periods increased phospho-AMPK and decreased phospho-S6K levels relative to ad libitum diets for genetic controls but not per^{01} mutants (Extended Data Fig. 5c, d). Next, we measured autophagic flux in control and *per* mutants on both ad libitum and iTRF diets using mCherry-tagged Atg8. The ratio of free mCherry to mCherry–Atg8a reflects autophagic activity because Atg8a is rapidly destroyed in the lysosome during autophagy while mCherry is more stable[29,30]. iTRF induced high levels of autophagy in controls relative to the ad libitum diet and significantly less in per^{01} mutants (Fig. 3d). Finally, we directly monitored autophagosome formation, lysosome abundance and autolysosome formation in the intestine via live fluorescence imaging of the autophagosome marker GFP–Atg8a relative to the lysosomal marker LysoTracker[30,31]. iTRF increased active autolysosomes in controls relative to the ad libitum diet but not in per^{01} mutants (Fig. 3e, Extended Data Fig. 5e). Thus, iTRF induction of autophagy correlates with lifespan extension and depends on the circadian clock.

To determine whether autophagy components are required for iTRF-mediated lifespan extension, we first manipulated autophagy-regulatory AMPK and TOR signalling pathways by driving expression of dominant-negative (DN) or constitutively active (CA) AMPK and S6K[32,33]. On an ad libitum diet, these known ageing regulators had expected effects, with pro-autophagy manipulations extending lifespan and autophagy inhibition shortening lifespan (Extended Data Fig. 6a–d, solid lines). On iTRF, while DN-S6K did not affect iTRF-mediated lifespan extension, DN-AMPK, CA-AMPK and CA-S6K partially inhibited iTRF-mediated lifespan extension (approximately 10%) relative to controls (more than 18%) (Extended Data Fig. 6a–d, dashed lines). Thus, in contrast to insulin signalling (Extended Data Fig. 2j), manipulation of these autophagy regulatory pathways affected iTRF-mediated lifespan.

To test the role of Atg1 and Atg8a directly, we knocked down *atg1* and *atg8a* expression using UAS-RNA interference (RNAi)-mediated knockdown via a ubiquitous inducible driver (*daughterless-GeneSwitch-GAL4*

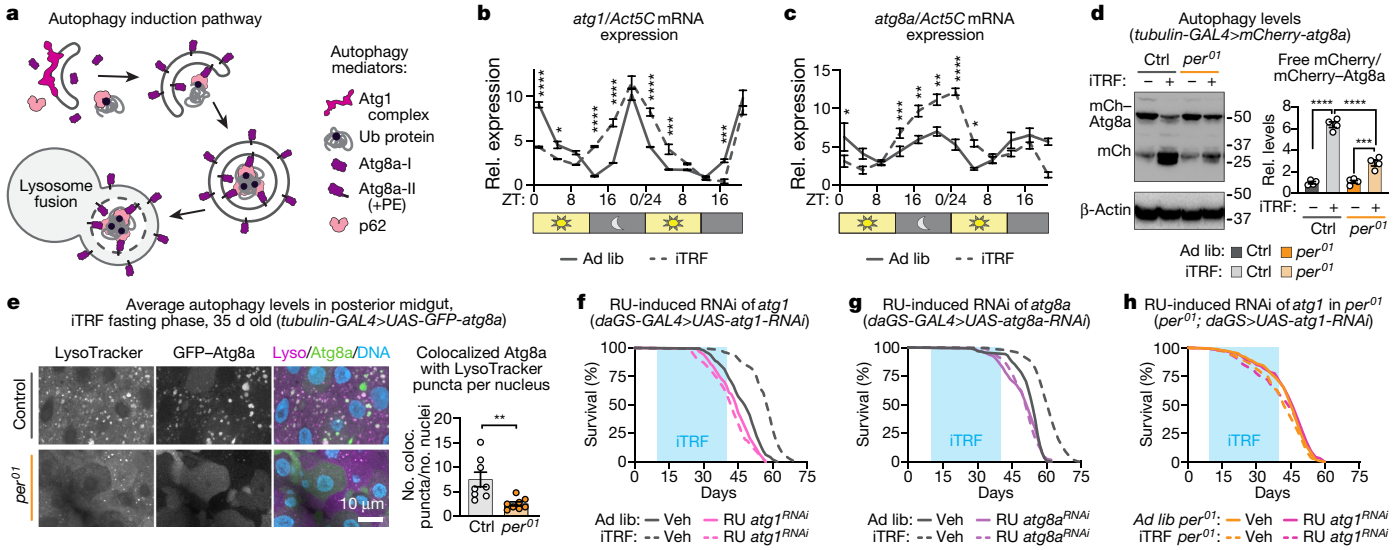

Fig. 3 | Autophagy mediators are required for iTRF-mediated lifespan extension. a, Schematic of core autophagy mediators. PE, phosphatidylethanolamine. **b**, **c**, *atg1* and *atg8a* expression were circadian-regulated; iTRF (dashed line) enhanced night-peaking *atg1* (**b**) and *atg8a* (**c**) expression relative to the ad libitum diet (solid line); each $n = 4$ biological replicates of 30 flies per condition per time point (unmarked is NS). **d**, iTRF (light grey) increased the ratio of free mCherry (mCh) to mCherry–Atg8a in controls relative to ad libitum (dark grey) and, to a lesser extent, in per^{01} mutants (ad libitum, orange; iTRF, light orange); each $n = 4$ biological replicates of 30 flies per genotype per condition. **e**, LysoTracker (magenta), GFP–Atg8a (green) and DNA (blue) staining revealed that control iTRF flies had increased autolysosomes in their intestines (light grey; $n = 8$ guts) compared with per^{01} mutants (light orange; $n = 8$ guts). **f**–**h**, The light blue boxes on graphs indicate the duration of iTRF. Relative to an ad libitum diet (solid lines), iTRF (dashed lines) extended the lifespans of controls (vehicle (Veh), grey; ad libitum $n = 195$ (**f**), $n = 169$ (**g**)); iTRF $n = 263$ (**f**), $n = 238$ (**g**)), but not flies with RNAi-mediated knockdown of *atg1* (pink; ad libitum $n = 158$, iTRF $n = 179$) (**f**) or *atg8a* (purple; ad libitum $n = 151$, iTRF $n = 152$) (**g**) in control backgrounds or in per^{01} backgrounds (per^{01} mutant, orange; ad libitum $n = 161$, iTRF $n = 167$; per^{01} mutant with *atg1*-RNAi, hot pink; ad libitum $n = 169$, iTRF $n = 174$) (**h**). See Methods and Supplementary Information for trials, statistics and source data; *n* refers to the number of flies unless otherwise specified; NS = $P > 0.05$, $^{*}P < 0.05$, $^{**}P < 0.01$, $^{***}P < 0.001$ and $^{****}P < 0.0001$; *P* values were obtained by ANOVA followed by Tukey's post-hoc test (**b**–**d**), unpaired, two-tailed *t*-test (**e**) and log-rank analysis (**f**–**h**). The centre values are the averages and the error bars indicate the s.e.m.).

(*daGS-GAL4*))[34]. This experiment also tested for developmental effects, as flies were fed the inducing drug RU486 or vehicle control starting at adult day 5. RNAi knockdown of *atg1* or *atg8a* in controls prevented iTRF-mediated lifespan extension (Fig. 3f, g) and *atg1* knockdown in per^{01} mutants had no effect (Fig. 3h). RU486 feeding alone did not affect lifespan extension of flies lacking UAS-RNAi transgenes (Extended Data Fig. 6e, f). Together, these data suggest that activation of autophagy is necessary for iTRF-mediated longevity.

iTRF requires circadian autophagy

To test whether circadian manipulation of autophagy impacts iTRF-mediated health benefits, we exploited circadian promoters and the UAS-GAL4 system[35] (Fig. 4a). We used *per-GAL4* and *tim-GAL4* (ref. [35]) to drive high night-time and low daytime expression of RNAi constructs against *atg1* and *atg8a*, respectively, confirming gene and protein expression by qRT–PCR and western blot analysis (Fig. 4b, Extended Data Fig. 7a). Flies with night-time RNAi knockdown of *atg1* or *atg8a* did not respond to iTRF (Extended Data Fig. 7b, c), suggesting that night-time *atg1* and *atg8a* expression are required for iTRF-mediated lifespan extension.

Because increased autophagy is known to extend lifespan[24], we tested whether circadian-regulated induction of autophagy with *per-GAL4* and *tim-GAL4*, driving *atg1* and *atg8a*, respectively, is sufficient for iTRF lifespan extension. The stronger *tim-GAL4* driver induced early lethality in combination with *atg1* (ref. [36]). Flies with night-specific overexpression of *atg1* or *atg8a* not only exhibited iTRF-like lifespan extension on an ad libitum diet but also exhibited no additional lifespan extension on iTRF (Fig. 4c, d). This suggests that, if circadian-regulated autophagy is already enhanced, iTRF has no effect. *tim-GAL4*-driven mCherry-tagged Atg8a expression had similar results (Extended Data Fig. 7d), and western blot analysis confirmed circadian oscillation of protein levels as well as induction of autophagy (Extended Data Fig. 7a). These results suggest that enhancing circadian-regulated autophagy is a major mechanism driving iTRF-mediated lifespan extension.

To confirm that lifespan extension reflects delayed ageing, we tested *atg1* RNAi and overexpression mutants and controls on ad libitum and iTRF diets for age-related declines in climbing ability and increased protein aggregation. Consistent with circadian *atg1* requirement for lifespan extension, circadian knockdown of *atg1* prevented iTRF-mediated healthspan extension (Extended Data Fig. 8a, b). Similarly, circadian overexpression of *atg1* caused iTRF-like healthspan extension in flies on an ad libitum diet, with no additional improvement on iTRF (Extended Data Fig. 8c, d). This suggests that circadian expression of *atg1* is both necessary and sufficient for iTRF-mediated lifespan and healthspan extension.

To pharmacologically enhance circadian-regulated expression, we used the RU486-inducible *daGS-GAL4* to overexpress *atg1* in flies on an ad libitum diet during the night/fasting phase (Fig. 4e, Extended Data Fig. 9a). Similar to *per-GAL4* driving *atg1*, night-specific RU486-induced overexpression of *atg1* was sufficient for iTRF-like lifespan extension on the ad libitum diet and inhibited further lifespan extension on iTRF (Fig. 4f). RU486-induced *atg1* overexpression in per^{01} mutants, which normally have lower iTRF-induced autophagy gene expression and function (Fig. 3d, e, Extended Data Fig. 5a–e), caused modest lifespan extension on both ad libitum and iTRF diets (Fig. 4g), suggesting that *atg1* expression in per^{01} mutants was not by itself sufficient for full response to iTRF.

Because night-specific RU486-induced autophagy was sufficient for iTRF-like lifespan extension, we tested day-specific RU486-induced autophagy. We developed a night-biased shifted 12:12 TRF regimen with 12-h fast (ZT9–ZT21) and 12-h feeding (ZT21–ZT9), without recovery

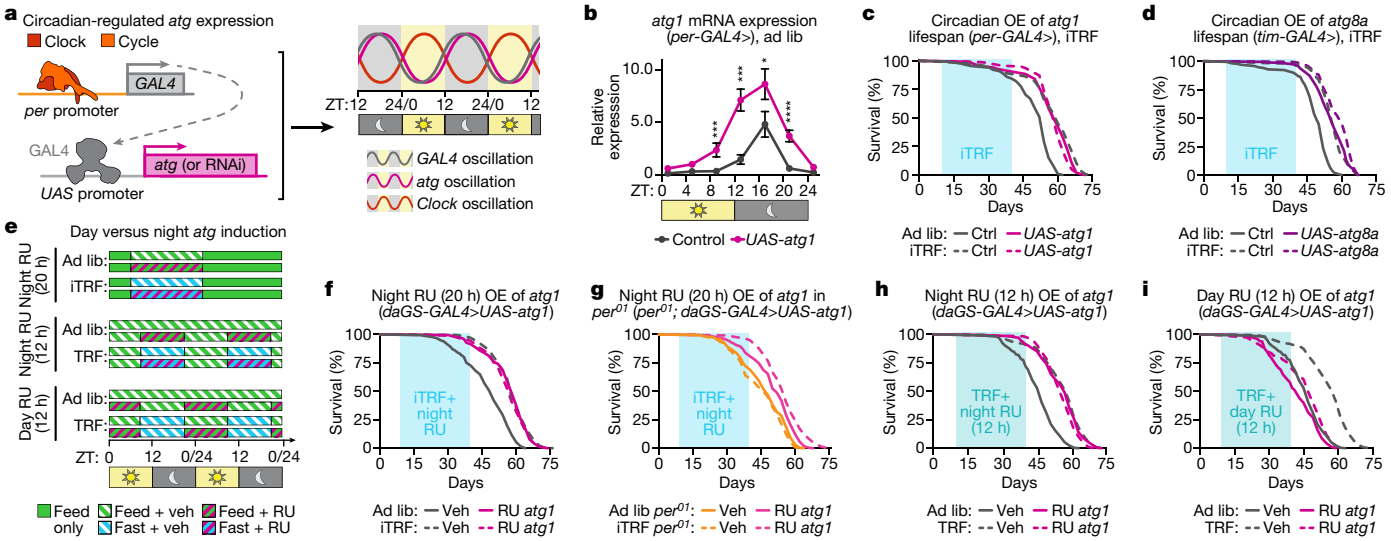

Fig. 4 | Increasing circadian-regulated expression of autophagy-promoting genes is sufficient for the health benefits of iTRF. a, Schematic of the genetic method to knockdown (or overexpress) autophagy components with circadian rhythmicity. **b**, *per-GAL4*-driven *atg1* expression (magenta line) enhanced circadian, night-peaking *atg1* gene expression (grey line); each $n = 4$ biological replicates of 30 flies per genotype per time point (unmarked is NS). **c**, **d**, Relative to controls (solid grey line, $n = 169–206$), genetic circadian overexpression (OE) of *atg1* (solid magenta line; $n = 139$) (**c**) or *atg8a* (solid purple line; $n = 191$) (**d**) caused lifespan extension on an ad libitum diet (solid lines) similar to controls on iTRF (dashed grey lines, $n = 139–263$) that was not further extended by iTRF (*atg1*, dashed magenta line, $n = 141$; *atg8a*, dashed purple line, $n = 228$). **e**, Schematic of pharmacological methods to overexpress *atg1* at different times of the day. **f**, RU486 (RU)-induced *atg1* overexpression at night extended lifespan of flies on an ad libitum diet (solid magenta line, $n = 197$) relative to controls on an ad libitum diet (solid grey line, $n = 186$), extending lifespan similar to controls on iTRF (dashed grey line, $n = 232$) and was not further extended by iTRF (dashed magenta line, $n = 329$). **g**, *atg1* overexpression extended lifespan less in per^{01} mutants (*per*: ad libitum, solid orange line, $n = 192$; iTRF, dashed orange line, $n = 245$; *per* with night *atg1* overexpression: ad libitum, solid pink line, $n = 225$; iTRF, dashed pink line, $n = 345$). **h**, **i**, Relative to controls on an ad libitum diet (solid grey line, $n = 208$), shifted TRF controls (dashed grey line, $n = 363$) and 12-h RU-induced overexpression of *atg1* (solid magenta line, $n = 236–290$) extended lifespan non-additively (dashed magenta line, $n = 192–341$) during the night phase (**h**) but not during the day phase (**i**). In **c**, **d**, **f**–**i**, the light blue boxes on graphs indicate the duration of iTRF (sky blue) or TRF (aqua) diets. See Methods and Supplementary Information for trials, statistics and source data; *n* indicates the number of flies unless otherwise specified; NS = $P > 0.05$, $^{*}P < 0.05$, $^{***}P < 0.001$ and $^{****}P < 0.0001$; *P* values were obtained by ANOVA followed by Tukey's post-hoc test (**b**), and log-rank analysis (**c**, **d**, **f**–**i**). The centre values are the averages and the error bars indicate s.e.m.).

days; the 3-h offset from lights off removed the evening meal and allowed sufficient fasting for robust lifespan extension similar to iTRF (Fig. 4e). Similar to this shifted 12:12 TRF, night-specific 12-h RU486 induction of *atg1* (ZT9–ZT21) produced iTRF-like lifespan extension that resisted further TRF lifespan extension (Fig. 4h). By contrast, day-specific fasting and/or RU486 treatment (ZT21–ZT9) did not extend lifespan (Fig. 4i). per^{01} mutants did not respond to shifted TRF (Extended Data Fig. 9b, c). These data suggest that night-specific enhanced *atg1* expression is both necessary and sufficient for iTRF-mediated lifespan extension (Extended Data Fig. 9d). Together, our results support the hypothesis that clock-dependent enhancement of macroautophagy mediates the effects of iTRF-mediated lifespan extension.

Both circadian regulation and autophagy control ageing and lifespan[28,37]. Here we identified circadian clock components (Tim, Per, Cyc and Clk) and essential autophagy components Atg1 and Atg8a as both necessary and sufficient for the anti-ageing, lifespan-extending benefits of iTRF. While a previous mouse study had found that TRF-mediated protection against high-fat diet did not require the circadian clock, a recent fly study confirmed our finding that iTRF-mediated lifespan extension requires a functional circadian clock[38]. With a diversity of cellular autophagy targets (proteins, lipids, nucleotides and organelles), identifying the major tissues and specific targets involved in iTRF-mediated, autophagy-associated health benefits are challenges for future work. Ageing is a major risk factor for mortality, triggering pathological processes that contribute to metabolic, cardiovascular and neurodegenerative diseases. As a simple dietary intervention strategy, iTRF appears to be both efficient and pleiotropic, with health benefits for multiple tissues, and offers a potential method of choice to combat ageing.

Online content

Any methods, additional references, Nature Research reporting summaries, source data, extended data, supplementary information, acknowledgements, peer review information; details of author contributions and competing interests; and statements of data and code availability are available at https://doi.org/10.1038/s41586-021-03934-0.

1. Longo, V. D. & Panda, S. Fasting, circadian rhythms, and time-restricted feeding in healthy lifespan. *Cell Metab.* **23**, 1048–1059 (2016).
2. Villanueva, J. E. et al. Time-restricted feeding restores muscle function in *Drosophila* models of obesity and circadian-rhythm disruption. *Nat. Commun.* **10**, 2700 (2019).
3. Chaix, A., Zarrinpar, A., Miu, P. & Panda, S. Time-restricted feeding is a preventative and therapeutic intervention against diverse nutritional challenges. *Cell Metab.* **20**, 991–1005 (2014).
4. Gill, S., Le, H. D., Melkani, G. C. & Panda, S. Time-restricted feeding attenuates age-related cardiac decline in *Drosophila*. *Science* **347**, 1265–1269 (2015).
5. de Cabo, R. & Mattson, M. P. Effects of intermittent fasting on health, aging, and disease. *N. Engl. J. Med.* **381**, 2541–2551 (2019).
6. Catterson, J. H. et al. Short-term, intermittent fasting induces long-lasting gut health and TOR-independent lifespan extension. *Curr. Biol.* **28**, 1714-1724.e4 (2018).
7. Manoogian, E. N. C. & Panda, S. Circadian rhythms, time-restricted feeding, and healthy aging. *Ageing Res. Rev.* **39**, 59–67 (2017).
8. Ja, W. W. et al. Prandiology of *Drosophila* and the CAFE assay. *Proc. Natl Acad. Sci. USA* **104**, 8253–8256 (2007).
9. Murphy, K. R., Park, J. H., Huber, R. & Ja, W. W. Simultaneous measurement of sleep and feeding in individual *Drosophila*. *Nat. Protoc.* **12**, 2355–2366 (2017).
10. Partridge, L., Alic, N., Bjedov, I. & Piper, M. D. W. Ageing in *Drosophila*: the role of the insulin/Igf and TOR signalling network. *Exp. Gerontol.* **46**, 376–381 (2011).
11. Cox, K. H. & Takahashi, J. S. Circadian clock genes and the transcriptional architecture of the clock mechanism. *J. Mol. Endocrinol.* **63**, R93–R102 (2019).
12. Dunlap, J. C. & Loros, J. J. Making time: conservation of biological clocks from fungi to animals. *Microbiol Spectr.* **5**, FUNK-0039-2016 (2017).
13. Allada, R. & Chung, B. Y. Circadian organization of behavior and physiology in *Drosophila*. *Annu. Rev. Physiol.* **72**, 605–624 (2010).

14. Panda, S. Circadian physiology of metabolism. *Science* **354**, 1008–1015 (2016).
15. Duong, H. A., Robles, M. S., Knutti, D. & Weitz, C. J. A molecular mechanism for circadian clock negative feedback. *Science* **332**, 1436–1439 (2011).
16. Xu, K., Zheng, X. & Sehgal, A. Regulation of feeding and metabolism by neuronal and peripheral clocks in *Drosophila*. *Cell Metab.* **8**, 289–300 (2008).
17. García-Gaytán, A. C. et al. Synchronization of the circadian clock by time-restricted feeding with progressive increasing calorie intake. Resemblances and differences regarding a sustained hypocaloric restriction. *Sci. Rep.* **10**, 10036 (2020).
18. Kinouchi, K. et al. Fasting imparts a switch to alternative daily pathways in liver and muscle. *Cell Rep.* **25**, 3299–3314.e6 (2018).
19. Wang, H. et al. Time-restricted feeding shifts the skin circadian clock and alters UVB-induced DNA damage. *Cell Rep.* **20**, 1061–1072 (2017).
20. Yamamuro, D. et al. Peripheral circadian rhythms in the liver and white adipose tissue of mice are attenuated by constant light and restored by time-restricted feeding. *PLoS ONE* **15**, e0234439 (2020).
21. Delventhal, R. et al. Dissection of central clock function in *Drosophila* through cell-specific CRISPR-mediated clock gene disruption. *eLife* **8**, e48308 (2019).
22. Ulgherait, M. et al. Circadian regulation of mitochondrial uncoupling and lifespan. *Nat. Commun.* **11**, 1927 (2020).
23. Ulgherait, M. et al. Dietary restriction extends the lifespan of circadian mutants tim and per. *Cell Metab.* **24**, 763–764 (2016).
24. Hansen, M., Rubinsztein, D. C. & Walker, D. W. Autophagy as a promoter of longevity: insights from model organisms. *Nat. Rev. Mol. Cell Biol.* **19**, 579–593 (2018).
25. Scott, R. C., Schuldiner, O. & Neufeld, T. P. Role and regulation of starvation-induced autophagy in the *Drosophila* fat body. *Dev. Cell* **7**, 167–178 (2004).
26. Kalfalah, F. et al. Crosstalk of clock gene expression and autophagy in aging. *Aging* **8**, 1876–1895 (2016).
27. Ma, D., Li, S., Molusky, M. M. & Lin, J. D. Circadian autophagy rhythm: a link between clock and metabolism? *Trends Endocrinol. Metab.* **23**, 319–325 (2012).
28. Rubinsztein, D. C., Mariño, G. & Kroemer, G. Autophagy and aging. *Cell* **146**, 682–695 (2011).
29. Chang, J. T., Kumsta, C., Hellman, A. B., Adams, L. M. & Hansen, M. Spatiotemporal regulation of autophagy during *Caenorhabditis elegans* aging. *eLife* **6**, e18459 (2017).
30. DeVorkin, L. & Gorski, S. M. Monitoring autophagy in *Drosophila* using fluorescent reporters in the UAS-GAL4 system. *Cold Spring Harb. Protoc.* **2014**, 967–972 (2014).
31. Ulgherait, M., Rana, A., Rera, M., Graniel, J. & Walker, D. W. AMPK modulates tissue and organismal aging in a non-cell-autonomous manner. *Cell Rep.* **8**, 1767–1780 (2014).
32. Mirouse, V., Swick, L. L., Kazgan, N., St Johnston, D. & Brenman, J. E. LKB1 and AMPK maintain epithelial cell polarity under energetic stress. *J. Cell Biol.* **177**, 387–392 (2007).
33. Barcelo, H. & Stewart, M. J. Altering *Drosophila* S6 kinase activity is consistent with a role for S6 kinase in growth. *Genesis* **34**, 83–85 (2002).
34. Tricoire, H. et al. The steroid hormone receptor EcR finely modulates *Drosophila* lifespan during adulthood in a sex-specific manner. *Mech. Ageing Dev.* **130**, 547–552 (2009).
35. Kaneko, M., Park, J. H., Cheng, Y., Hardin, P. E. & Hall, J. C. Disruption of synaptic transmission or clock-gene-product oscillations in circadian pacemaker cells of *Drosophila* cause abnormal behavioral rhythms. *J. Neurobiol.* **43**, 207–233 (2000).
36. Plautz, J. D., Kaneko, M., Hall, J. C. & Kay, S. A. Independent photoreceptive circadian clocks throughout *Drosophila*. *Science* **278**, 1632–1635 (1997).
37. Duffy, J. F., Zitting, K.-M. & Chinoy, E. D. Aging and circadian rhythms. *Sleep Med. Clin.* **10**, 423–434 (2015).
38. Cabrera, D., Young, M. W. & Axelrod, S. Time-restricted feeding prolongs lifespan in *Drosophila* in a peripheral clock-dependent manner. Preprint at *bioRxiv* https://doi.org/10.1101/2020.09.14.296368 (2020).

Methods

Fly strains

w^{1118} *Canton-S* (*CS*) were used as a 'wild-type' strain throughout this paper. *UAS-DN-S6K* (6911), *UAS-CA-S6K* (6914), *UAS-DN-AMPK* (32112), *UAS-CA-AMPK* (32110), *UAS-atg1*-RNAi (44034), *UAS-atg8a*-RNAi (34340) and *UAS-atg1* (51654) were obtained from the Bloomington Stock Center and outcrossed to *CS* for at least 10 generations. *tubulin-GAL4* flies were obtained from J. Carlson, *UAS-mCh-atg8a* and *UAS-GFP-atg8a* from E. Baehrecke, and *daGS* from D. W. Walker; all were outcrossed to *CS* for at least 10 generations. *period* (per^{01}) mutants, *timeless-GAL4* and *period-GAL4* were obtained from J. Giebultowicz and, because they were last outcrossed many years ago, were outcrossed to *CS* for 12 generations in the past 2 years. *UAS*-gRNA and *UAS-CAS9* lines were those utilized in our previous papers and were outcrossed to *CS* for five generations[22,39]. Previously outcrossed *cycle* (cyc^{01}) mutants were obtained from S. Syed with a *CS* control strain. All experiments with multiple transgenes used flies that had undergone 12 generations of out-crossing into a *CS* control and/or per^{01}, *CS* mutant background.

Fly media

Developmental media consisted of standard yeast-cornmeal-agar media (Archon Scientific, glucose recipe: 7.6% w/v glucose, 3.8% w/v yeast, 5.3% w/v cornmeal, w/v 0.6% agar, 0.5% v/v propionic acid, 0.1% w/v methyl paraben and 0.3% v/v ethanol). Adult flies that eclosed within a 24-h period were collected and transferred to 'adult medium' containing 4% glucose, 2% sucrose, 8% cornmeal, 1% agar, and either 0%, 0.5%, 1%, 2%, 3%, 6% or 10% yeast extract (Difco) supplemented with 1.5% methylparaben mix (10% methylparaben dissolved in ethanol) and 1% propionic acid for lifespan and biochemical analysis. Food for ad libitum, iTRF, TRF and shifted TRF diets was adult medium with 3% yeast extract. All percentages are given in w/v except the methylparaben mix, and propionic acid is given in v/v. Fasting media consisted of 1% agar in ddH_2O made fresh daily. Food for activity recording CAFE (ARC) assays is described below.

Drug supplementation in media for lifespan

All drugs were supplemented into cooled (65 °C) liquid adult medium (containing 3% yeast extract) following preparation to the following final concentration(s); for RNAi experiments, RU486 (Cayman Chemical) was dissolved in ethanol and supplemented into medium after day 5 post-eclosion at a final concentration of 100 μg/ml; vehicle controls were supplemented with the same volume of ethanol alone. Timed RU486 feeding of *daGS>UAS-atg1* consisted of flies being fed 0.5 μg/ml in standard adult media or fasting media only during the fasting phase, then flipped to vehicle control food the following morning only from days 10 to 40 of adulthood. Vehicle-only controls were flipped at the same time for consistency. For gut microorganism clearance, the medium contained 500 μg/ml ampicillin, 50 μg/ml tetracycline and 200 μg/ml rifamycin in 50% ethanol and the same volume of 50% ethanol alone was used as the vehicle control.

Lifespan analysis

Drosophila were reared from embryos in low-density bottles with standard yeast-cornmeal-agar media listed above (Archon Scientific). Newly eclosed flies (approximately 24 h post-eclosion) were collected onto adult medium with 3% yeast extract and allowed to mate for 48 h. Female and male flies were separated and maintained at a density of 30–35 flies per vial in a humidified (65%), temperature-controlled (25 °C) incubator with a 12-h light–dark cycle. All flies were raised on ad libitum conditions until day 10 post-eclosion upon which flies were placed on various feeding regimes (Extended Data Fig. 1a). For consistency, ad libitum control flies were flipped on to fresh food at the same time as experimental diet flies were transferred to fasting media, and once again when fasting flies were flipped on to regular adult media. Death was scored at time of flipping, and lifespan was compared by log-rank analysis.

ARC assay

Feeding data from individual flies were collected as previously described[9,40]. Feeding medium was a solution of 4% dextrose, 2% sucrose and 3% yeast extract in ddH_2O, filtered (with a 0.2-μm cellulose acetate sterile syringe filter; VWR). Flies were transferred to fresh standard medium every other day until the experiment. When the flies were 9–11 days old, the animals were loaded by mouth pipette into standard ARC chambers and allowed to acclimate overnight (approximately 18 h) with access to the test diet in a glass capillary pipette. The capillaries were replaced daily with those containing fresh food or ddH_2O. The meniscus level of each capillary was tracked for the entire duration of the feeding periods at 1-s intervals. Drops in meniscus position above a pre-calibrated threshold were considered feeding events, and feeding bouts less than 2 min apart were considered to be part of the same meal. The volume consumed from each feeding event was automatically calculated and collated with a custom Python code[9,40].

Intestinal barrier dysfunction 'smurf' assay

The 'smurf fly' intestinal barrier dysfunction assay was performed as previously described[41,42]. Flies were aged on standard adult medium (see 'Fly media') until the day of the smurf assay. Dyed medium was prepared by the addition of FD&C Blue No. 1 at a final concentration of 2.5% w/v. A fly was counted as a smurf when dye colouration was observed outside the digestive tract. Comparisons of smurf proportion per time point were carried out using binomial tests to calculate the probability of having as many smurfs in population A as in population B, as well as analysis of variance (ANOVA) for proportions of smurf flies per replicate vial with a minimum of 7 vials of 12–31 flies per replicate.

qRT–PCR

Female flies (35 days old) on either ad libitum or iTRF conditions were collected for RNA extraction over the course of 48 h in 4-h intervals. Four biological replicates of 30 female flies per time point and feeding regimen were snap-frozen in liquid nitrogen and stored at −80 °C. RNA was extracted using TRIzol (Invitrogen) following the manufacturer's protocol. Samples were treated with DNaseI (Invitrogen), then heat inactivated. cDNA was synthesized by the Revertaid First Strand cDNA Synthesis Kit (Thermo Scientific). PowerUp SYBR Mastermix (Applied Biosystems) was used to perform qRT–PCR using a CFX-Connect thermal cycler (Bio-Rad). Primer efficiency and relative quantification of transcripts were determined using a standard curve of serial diluted cDNA. Transcripts were normalized using *Act5C* as a reference gene. The Jonckheere–Terpstra–Kendall (JTK) algorithm was applied using the JTK-Cycle package in R software[43] to determine significance of rhythmic cycling. Differences between individual time points were determined by ANOVA followed by multiple comparison tests.

qRT–PCR primers: *period* (forward): GGTTGCTACGTCCTTCTGGA; *period* (reverse): TGTGCCTCCTCCGATATCTT; *timeless* (forward): CCGTGGACGTGATGTACCGCAC; *timeless* (reverse): CGCAATGGGCATGCGTCTCTG; *clock* (forward): GGATAAGTCCACGGTCCTGA; *clock* (reverse): CTCCAGCATGAGGTGAGTGT; *atg1* (forward): GCTTCTTTGTTCACCGCTTC; *atg1* (reverse): GCTTGACCAGCTTCAGTTCC; *atg8a* (forward): AGTCCCAAAAGCAAACGAAG; *atg8a* (reverse): TTGTCCAAATCACCGATGC; *actin5C* (forward): TTGTCTGGGCAAGAGGATCAG; *actin5C* (reverse): ACCACTCGCACTTGCACTTTC; *16Sr* (forward): AGAGTTTGATCCTGGCTCAG; *16Sr* (reverse): CTGCTGCCTYCCGTA.

Microbial load quantification

For 16S bacterial rDNA quantification, 4 replicates of 10 whole flies (washed twice in 70% ethanol and twice in PBS) were used for total DNA extraction via the Power Soil DNA isolation kit (Qiagen). Universal primers for the 16S ribosomal RNA gene were against variable regions 1 (V1F) and 2 (V2R), as previously published[44].

Western blot analysis

Whole-body lysates of female flies (30 flies per genotype per condition per time point) were separated by SDS–PAGE using standard procedures. Membranes were probed with antibodies against AMPK phospho-T184 at 1:1,000 dilution (40H9, Cell Signaling), anti-phospho-S6K T398 (9209, Cell Signaling), mCherry (E5D8F, Cell signaling) and horseradish peroxidase (HRP)-conjugated monoclonal mouse anti-actin antibody at 1:5,000 dilution (A3854, Sigma-Aldrich). Rabbit antibodies were detected using HRP-conjugated anti-rabbit IgG antibodies at 1:2,000 dilution (7074, Cell Signaling). Mouse antibodies were detected using HRP-conjugated anti-mouse IgG antibodies at 1:2,000 dilution (7076, Cell Signaling). ECL chemiluminescence reagent (Pierce) was used to visualize HRP activity and detected by a CCD camera Bio-Rad image station. A minimum of four independent samples of each condition were used for statistical analysis and quantification.

Immunostaining of indirect flight muscle

Immunofluorescence was performed as previously described[45]. Hemithoraces were dissected and fixed for 20 min in PBS with 4% paraformaldehyde and 0.1% Triton X-100. After washing, samples were incubated overnight at 4 °C with an antibody against poly-ubiquitylated proteins, the mouse monoclonal antibody FK2 (Enzo) and anti-P62 rabbit ab178440 (Abcam) at 1:200 dilutions, then washed thoroughly and incubated with secondary anti-mouse AlexaFluor-488 (1:250), anti-rabbit AlexaFluor-555 (1:250) and phalloidin AlexaFluor-647 (1:150) (all Invitrogen). Samples were rinsed three times in PBS with 0.1% Triton X-100 for 10 min at room temperature, then mounted in Prolong Gold (Invitrogen) and imaged via confocal microscopy using ×20 dry objective with 0.5 numerical aperture (NA) (LSM-800 Zeiss, standard laser lines: 405, 488, 561 and 640 nm). Identical laser power settings and photomultiplier values were used for imaging between conditions. For quantification of protein aggregates of hemithoraces, the size and area of protein aggregates were measured using ImageJ particle counter software (ImageJ version 2.0.0-rc-69/1.52p)[46]. Statistical analysis was conducted using a two-tailed, unpaired Student's *t*-test or ANOVA followed by Tukey's multiple comparisons ($n \geq 9$ thoraces per condition).

Climbing activity

Assessment of climbing ability was performed as previously described[47] with minor modifications. Briefly, 10 flies were transferred to an empty standard 23 mm × 95 mm plastic vial and then gently tapped to the bottom. The number of flies that reached the top quarter of the vial within 20 s was then scored as climbing. Each experiment was performed on a minimum of 8 vials of 10 flies per condition repeated three times.

LysoTracker Red staining

Female flies (35 days old) near the end of a 20-h fasting phase were anaesthetized on ice and intestines were dissected in cold PBS. Intestines were washed once in PBS, followed by three 30-s rinses in freshly prepared 1 μM LysoTracker Red, (Invitrogen) and 1.5 μg/ml Hoechst stain in PBS at room temperature. Intestines were washed five times for 30 s in PBS at room temperature, then mounted in Vectashield (Vector Labs) and imaged immediately. Imaging was conducted using a ×63 oil objective with 1.4 NA on a Zeiss LSM-800 with standard laser lines (405, 488, 561 and 640 nm) and using identical power settings between samples. Imaging should not proceed for very long as apoptosis can be observed after approximately 60 min. Colocalization GFP–Atg8a quantification was conducted in the COLOC2 plugin for ImageJ (ImageJ version 2.0.0-rc-69/1.52p)[46]. The number of vesicles with significant LysoTracker and GFP–Atg8a colocalization determined by significant Pearson's correlation coefficient was then counted using the ImageJ[46] particle counter tool (ImageJ version 2.0.0-rc-69/1.52p). Similarly, the total number of LysoTracker-labelled and GFP–Atg8a vesicles was determined using the ImageJ[46] particle counter tool (ImageJ version 2.0.0-rc-69/1.52p). Statistical analysis was conducted using a two-tailed, unpaired Student's *t*-test.

Triton-insoluble protein extracts

Flies were homogenized in ice-cold PBS with 1% Triton X-100 and protease inhibitor cocktail (Roche). The mixture was spun for 10 min at 4 °C, and the pellet and supernatant were collected. The Triton X-100-insoluble pellet was washed in one additional volume of Triton X-100 solution and resuspended in denaturing lysis solution with 5% lithium dodecyl sulfate (LDS) containing 300 mM dithiothreitol (NuPAGE LDS Sample Buffer; Invitrogen). $n = 4$ independent samples of 30 flies were used for post-western blot densitometry analysis.

Phospho-histone H3 immunostaining

Briefly, flies were anaesthetized on ice and intestines were dissected in cold PBS. Samples were then fixed in PBS plus 0.1% Triton X-100 containing 4% paraformaldehyde at room temperature for 30 min and rinsed three times in PBS plus 0.1% Triton X-100 for 10 min at room temperature. Blocking was performed in 5% BSA in PBS plus 0.1% triton X-100 for 1 h at room temperature. Primary antibody, anti-phospho-histone H3 (S10) (9701, Cell Signaling), was added at 1:250 in 5% BSA in PBS plus 0.1% Triton X-100 and incubated overnight at 4 °C rotating. After washing three times in PBS plus 0.1% Triton X-100 secondary antibody, anti-rabbit AlexaFluor-488 (Invitrogen) was added at 1:250 dilution with 1.5 μg/ml Hoechst stain (Thermo) in 5% BSA in PBS plus 0.2% Triton X-100 and incubated overnight at 4 °C rotating. After washing, intestines were then mounted in Vectashield mounting medium (Vector Labs) and imaged using a ×20 dry objective on a Zeiss LSM-800 with 0.5 NA and standard laser lines (405, 488, 561 and 640 nm) and using identical power settings between samples. Phospho-histone H3-positive cells were quantified using the ImageJ[46] local maxima tool, with identical thresholding for all images (ImageJ version 2.0.0-rc-69/1.52p). Phospho-histone H3 numbers were normalized to the area of the posterior midgut imaged. A minimum of eight intestines were used for each quantification.

Statistical analysis and replicability

Initial lifespan screens were blinded to researchers by number assignment. Repeat experiments were not blinded, but mortality values were counted by impartial undergraduate researchers. Prism7 (GraphPad) was used to perform the statistical analysis. Significance is expressed as *P* values (NS = $P > 0.05$, $^{*}P < 0.05$, $^{**}P < 0.01$, $^{***}P < 0.001$ and $^{****}P < 0.0001$). For comparison of two groups, unpaired, two-tailed *t*-test was used, when data met criteria for parametric analysis (normal distribution and similar variance). For comparison of more than two groups, ANOVA with Bonferroni, or Tukey's post-hoc test was performed. Kruskal–Wallis with Dunn's post-hoc analysis was used for non-parametric data. All plotted values represent means, with error bars representing s.e.m. All biochemical experiments were performed with a minimum of four biological replicates, repeated in two to three independent trials. For comparison of survival curves, log-rank (Mantel–Cox) analysis was used. For ad libitum versus iTRF (day 10–40) comparisons on 3% yeast extract, control flies (w1118, Canton S) were tested nine times, either as experimentals or as controls for other experiments (Figs. 1b, d, 2d, plus two repeats, 2f, Extended Data Figs. 3j, 4c plus repeat, Extended Data Fig. 4e). per^{01} mutants were tested four times (Fig. 2f, Extended Data Fig. 4c plus repeat, Extended Data Fig. 4e); *per* and *tim* CRISPR mutants were each tested twice (Fig. 2e plus repeat), clk^{JRK} mutants were tested three times (Fig. 2d plus two repeats) and cyc^{01} mutants were tested four times (Extended Data Fig. 4b plus two repeats, Extended Data Fig. 4e). All other lifespans with genetic manipulations were tested two times, with the exception of large screens of alternative diets such as protein titrations (Fig. 1d, Extended Data Fig. 4d, e), alternative TRFs (Extended Data Fig. 1b–f), time windows for iTRF (Extended Data Fig. 2a–g), antibiotic treatment (Extended Data Fig. 3i, j), or night versus day bias (Figs. 2f, 4h, i,

Extended Data Fig. 9b, c), as well as mCherry–Atg8 controls (Extended Data Fig. 7d) and *daGS* driver controls (Extended Data Fig. 6g, g), which were tested once. Titration of protein and lifespan with per^{01} mutants has been previously published[23]. See Supplementary Table 1 for details of all lifespan trials and Supplementary Table 2 for raw source data.

Reporting summary

Further information on research design is available in the Nature Research Reporting Summary linked to this paper.

Data availability

The authors declare that all data supporting the findings of this study are available, including replicate experiments, and will be made available on reasonable request from the corresponding author.

39. Delventhal, R. et al. Dissection of central clock function in *Drosophila* through cell-specific CRISPR-mediated clock gene disruption. *eLife* **8**, e48308 (2019).
40. Murphy, K. R. et al. Postprandial sleep mechanics in *Drosophila*. *eLife* **5**, e19334 (2016).
41. Rera, M., Clark, R. I. & Walker, D. W. Intestinal barrier dysfunction links metabolic and inflammatory markers of aging to death in *Drosophila*. *Proc. Natl Acad. Sci. USA* **109**, 21528-21533 (2012).
42. Rera, M. et al. Modulation of longevity and tissue homeostasis by the *Drosophila* PGC-1 homolog. *Cell Metab.* **14**, 623-634 (2011).
43. Hughes, M. E., Hogenesch, J. B. & Kornacker, K. JTK_CYCLE: an efficient nonparametric algorithm for detecting rhythmic components in genome-scale data sets. *J. Biol. Rhythms* **25**, 372-380 (2010).
44. Claesson, M. J. et al. Comparison of two next-generation sequencing technologies for resolving highly complex microbiota composition using tandem variable 16S rRNA gene regions. *Nucleic Acids Res.* **38**, e200 (2010).
45. Rana, A., Rera, M. & Walker, D. W. Parkin overexpression during aging reduces proteotoxicity, alters mitochondrial dynamics, and extends lifespan. *Proc. Natl Acad. Sci. USA* **110**, 8638-8643 (2013).
46. Schneider, C. A., Rasband, W. S. & Eliceiri, K. W. NIH Image to ImageJ: 25 years of image analysis. *Nat. Methods* **9**, 671-675 (2012).
47. Copeland, J. M. et al. Extension of *Drosophila* life span by RNAi of the mitochondrial respiratory chain. *Curr. Biol.* **19**, 1591-1598 (2009).

Acknowledgements We thank all members of the Shirasu-Hiza and Canman laboratories for support, discussions and feedback. We also thank D. W. Walker and J. Giebultowicz for fly lines. Other stocks were obtained from the Bloomington *Drosophila* Stock Center (NIH P40OD018537). Work was supported by Charles H. Revson Foundation (to M.U.), AFAR Glenn Foundation Postdoctoral Fellowship for Aging Research (to M.U.), Celia Lipton Farris and Victor W. Farris Foundation Graduate Student Fellowship (to S.J.P.), NIH T32GM007088 (to J.G.), NIH R01GM117407 (to J.C.C.), NIH R01GM130764 (to J.C.C.), Joe W. and Dorothy Dorsett Brown Foundation (to W.W.J.), NIH R56AG065986 (to W.W.J.), NIH R35GM127049 (to M.S.-H.) and NIH R01AG045842 (to M.S.-H.).

Author contributions M.U. and M.S.-H. conceived the experiments. Experiments were performed and analysed by M.U. (all), A.M.M. (lifespan experiments), S.J.P. and W.W.J. (feeding analysis), J.G. (western blots and lifespan experiments), S.J.T. (qRT–PCR and lifespan experiments), J.S. (lifespan experiments) and N.K. (biochemical and imaging experiments, and western blots). M.U., J.C.C. and M.S.-H. made intellectual contributions, designed the figures and wrote the manuscript.

Competing interests The authors declare no competing interests.

Additional information

Supplementary information The online version contains supplementary material available at https://doi.org/10.1038/s41586-021-03934-0.

Correspondence and requests for materials should be addressed to Mimi Shirasu-Hiza.

Peer review information *Nature* thanks Tor Erik Rusten and the other, anonymous, reviewer(s) for their contribution to the peer review of this work.

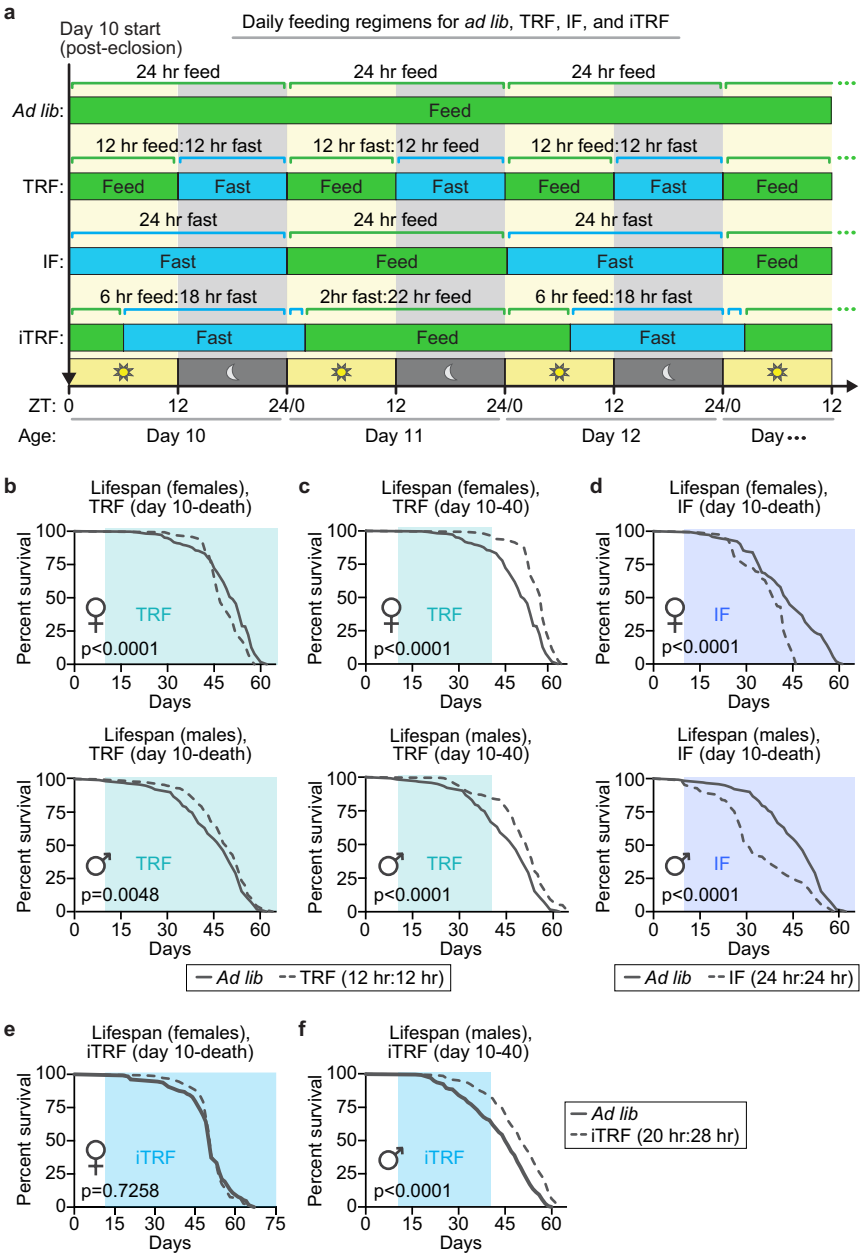

Extended Data Fig. 1 | Lifespan changes in response to different feeding and fasting regimens. Light blue boxes on graphs indicate duration of TRF (aqua), IF (medium blue), or iTRF (sky blue) during lifespan. **a**, Schematic of different feeding regimens utilized in *Drosophila* lifespan screen. **b**, 12-hour time-restricted feeding (TRF) from day 10 until death shortened female lifespan (top; *ad lib*, solid gray, n=292; TRF, dashed gray, n=142) and minimally extended male lifespan (bottom; *ad lib*, solid, n=241; TRF, dashed, n=314). **c**, In contrast, TRF from days 10-40 extended female (top; *ad lib*, solid gray, n=292; TRF, dashed gray, n=150) and male (bottom; *ad lib*, solid gray, n=241; TRF, dashed gray, n=406) lifespan. **d**, 24-hour intermittent fasting (IF) from day 10-death shortened both female (top; *ad lib*, solid gray, n=145; IF, dashed gray, n=149) and male (bottom top; *ad lib*, solid gray, n=241; IF, dashed gray, n=276) lifespan. **e**, Intermittent time-restricted feeding (iTRF) from day 10-death did not extend lifespan (*ad lib*, solid gray, n=142; TRF, dashed gray, n=157). **f**, iTRF regimen from days 10-40 extended male lifespan (*ad lib*, solid gray, n=323; TRF, dashed gray, n=382). (See Methods and SI for trials, statistics, and source data; n=number of individual flies; p-values were obtained by log-rank analysis (**b**–**f**).

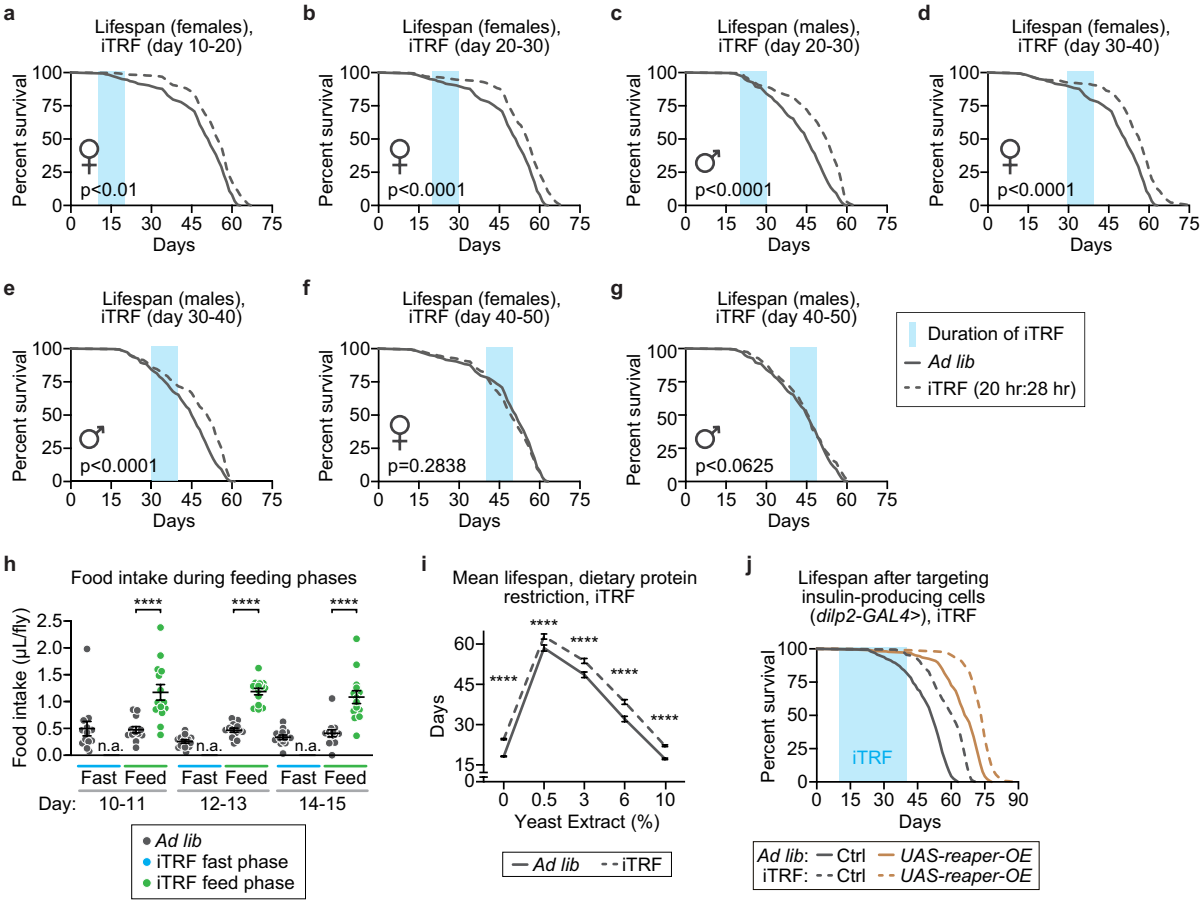

Extended Data Fig. 2 | Characterization of iTRF windows and effect on feeding and dietary restriction. Light blue boxes on graphs indicate duration of iTRF during lifespan; solid and dashed lines represent flies on *ad lib* and iTRF diets, respectively. **a**–**e**, 10-day periods of iTRF in early to mid-life (days 10-40 of adulthood) can extend lifespan but not later in life (days 40-50): (**a**) days 10-20 with females (*ad lib* n=311; iTRF n=319); days 20-30 with (**b**) females (iTRF n=337) and (**c**) males (*ad lib* n=323; iTRF n=366); days 30-40 with (**d**) females (iTRF n=355) and (**e**) males (iTRF n=293) all extend lifespan. **f**, **g**, iTRF days 40-50 of adulthood did not extend male (iTRF n=302) or female (iTRF n=349) lifespan. **h**, Relative to flies on *ad lib* diet (dark gray dots, n=13), flies on iTRF (shown as blue or green dots depending on diet phase, n=14) starve during the fasting phase (n.a., no food available) and eat more during the feeding phase (green dots). **i**, iTRF extended mean lifespan regardless of dietary protein concentration (n=98-347 for each sample of *ad lib* or iTRF flies at each protein concentration). **j**, After partial genetic ablation of insulin producing cells, iTRF still extended lifespan (dashed brown, n=424) relative to *ad lib* diet (solid brown, n=310), to a similar extent as in genetic controls (*ad lib*, solid gray, n=161; iTRF, dashed gray, n=180). (See Methods and SI for trials, statistics, and source data; n=number of individual flies; ****=p<0.0001; p-values were obtained by log-rank analysis (a-g, and j) and unpaired two-tailed t-test (h-i). Center values=averages; error bars=SEM.).

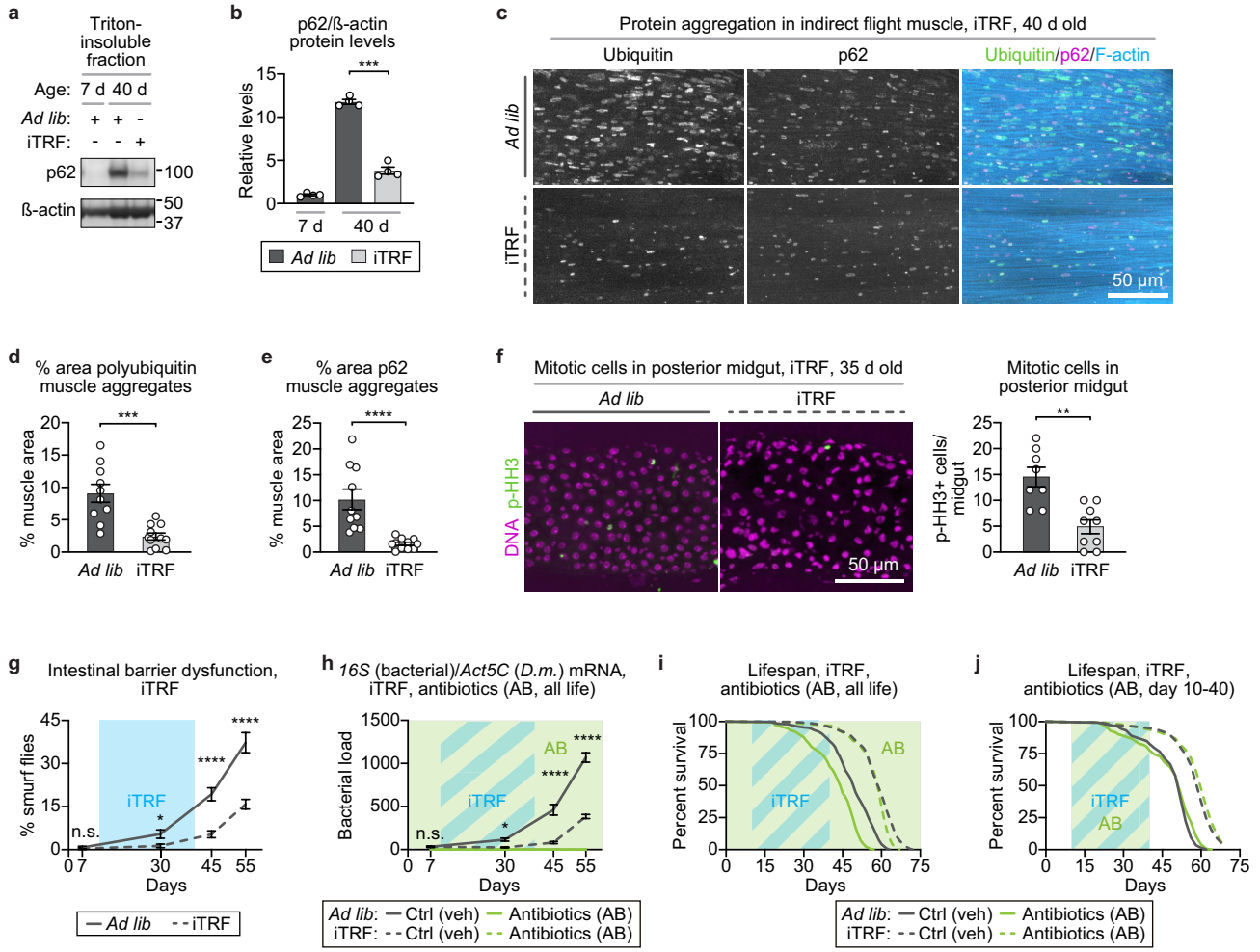

Extended Data Fig. 3 | iTRF delays aging markers (protein aggregation and intestinal dysfunction) and extends lifespan independent of microbiota. **a**, Representative western blot of Triton-insoluble protein accumulation of p62/ref(2)P (each sample=30 flies/condition/timepoint; see also Supplementary Fig. 1). **b**, Quantification of triton insoluble protein levels showed that iTRF flies (light gray) exhibited reduced accumulation of p62/ref(2)P with age, relative to *ad lib* flies (dark gray) (average of 4 biological repeats). **c**, Representative images of 40-day old indirect flight muscle stained for polyubiquitin protein aggregates (green), p62/ref(2)P (magenta), and filamentous actin (F-actin, blue); scale bar=50 µm. **d**, **e**, iTRF significantly reduced (**d**) polyubiquitin aggregates and (**e**) accumulation of p62 aggregates (*ad lib* n=10 thoraces, iTRF n=11 thoraces). **f**, iTRF also reduced age-related intestinal over-proliferation, as marked by phospho-histone H3 staining (p-HH3) (*ad lib* n=8 guts; iTRF n=9 guts); scale bar=50 µm. **g**, Light blue boxes on graphs indicate duration of iTRF during lifespan. iTRF (dashed line) delayed age-related intestinal barrier dysfunction relative to *ad lib* (solid line), as marked by decreased numbers of smurf flies (n=8-12 cohorts of 20-31 flies). **h**–**j**, Light colored boxes on graphs indicate duration of antibiotic treatment (AB, green) or antibiotic treatment plus iTRF diet (blue/green striped) during lifespan. iTRF flies showed delayed age-related growth in microbiome load with age (n=30 flies/condition/timepoint, 4 biological replicates) (**h**). iTRF extended lifespan upon microbiome clearance via antibiotics treatment during either (**i**) total lifespan (*ad lib* n=227, iTRF n=268) or (**j**) only days 10-40 of adulthood (*ad lib* n=144, iTRF n=190). (See Methods and SI for trials, statistics, and source data; n=number of flies unless otherwise indicated; n.s.=p>0.05, *=p<0.05, **=p<0.01, ***=p<0.001, ****=p<0.0001; p-values were obtained by ANOVA followed by Tukey's post-hoc test (**b**, **g**, **h**), unpaired two-tailed student's t-test (**d**–**f**), and log-rank analysis (**i**, **j**). Center values=averages; error bars=SEM.).

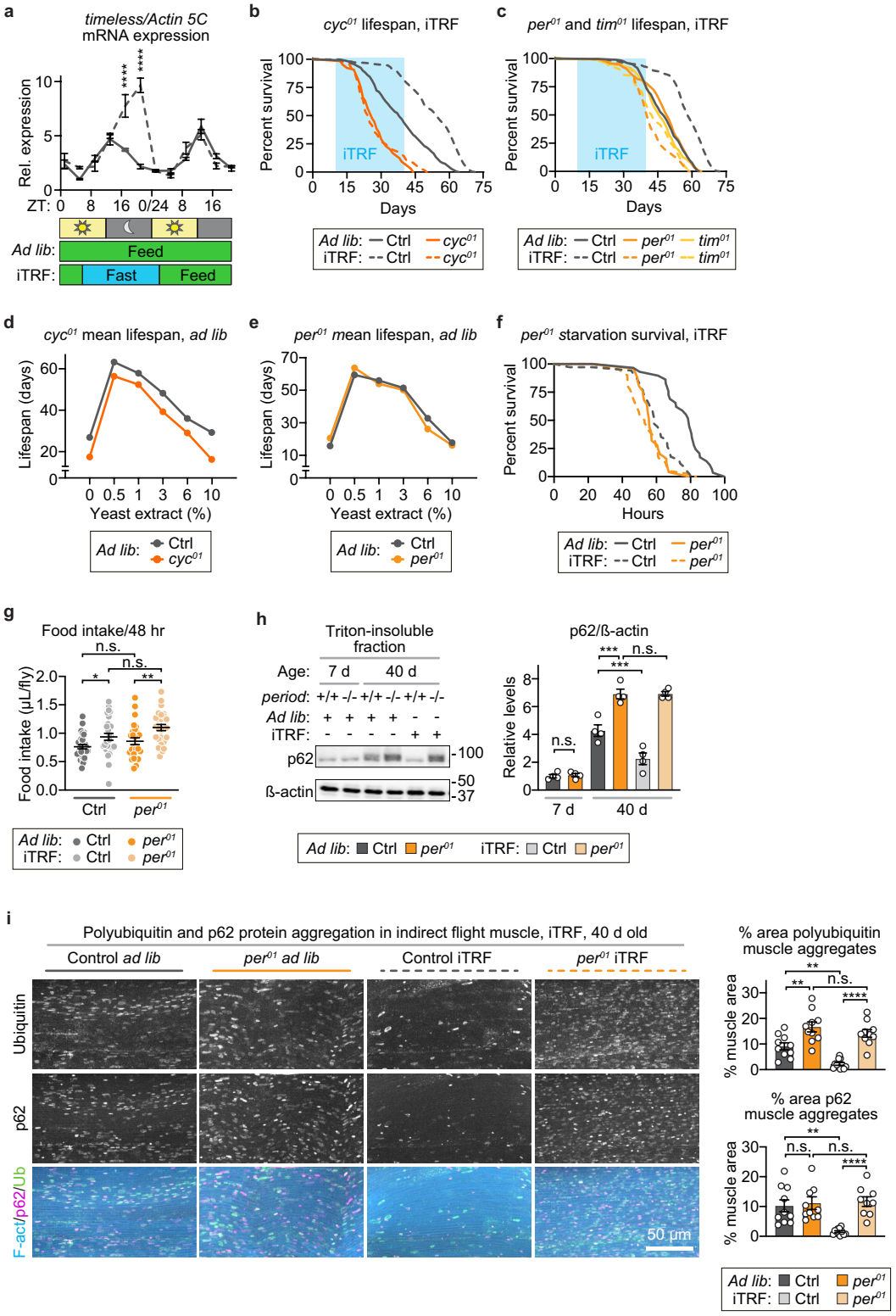

Extended Data Fig. 4 | See next page for caption.

Extended Data Fig. 4 | Circadian mutants show a normal lifespan response to dietary protein restriction but do not respond to iTRF. a, Gene expression of *timeless*, similar to *period* and *Clock*, was enhanced by iTRF during the fasting phase (each n=4 biological replicates of 30 female flies/genotype/condition/timepoint; unmarked=n.s.). **b**, **c**, Light blue boxes on graphs indicate duration of iTRF during lifespan. Circadian mutants did not respond to iTRF with extended lifespan relative to controls (*ad lib* n=187-288; iTRF n=290-311): (**b**) $cycle^{01}$ (*ad lib* n=65, iTRF n=121) and (**c**) $timeless^{01}$ (*ad lib* n=120, iTRF n=152) and $period^{01}$ (*ad lib* n=215, iTRF n=184) null mutant females did not respond to iTRF with extended lifespan. **d**, **e**, (**d**) $cycle^{01}$ and (**e**) $period^{01}$ mutant females showed a normal "tent-curve" lifespan response to dietary protein titration (n=61-272 flies/genotype/condition/timepoint). **f**, $period^{01}$ mutant females did not starve significantly faster than controls whether they have been on iTRF or *ad lib* diet (controls: *ad lib* n=31, iTRF n=35; *per*: *ad lib* n=27, iTRF n=42). **g**, Similar to controls (gray, *ad lib* n=30; light gray, iTRF, n=29), $period^{01}$ mutant females (orange, *ad lib* n=27; light orange, iTRF, n=27) ate more on iTRF relative to on *ad lib* diet. **h**, Unlike control iTRF flies (light gray), which had reduced accumulation of p62/ref(2)P with age relative to *ad lib* flies (dark gray), *per* mutants had similar levels on *ad lib* (orange) or iTRF (light orange) diets (each dot=1 sample=30 flies; each bar=average of 4 biological repeats). Actin blot is repeated from Fig. 2h because the same western blot was used to quantify Ubiquitin, p62/ref(2)P, and actin (loading control); see also Supplementary Fig. 1. **i**, Representative images of indirect flight muscle from 40-day-old flies stained for filamentous actin (F-actin, blue), ubiquitin (green), and p62/ref(2)P (magenta) showed that, unlike genetic controls (*ad lib* n=10, iTRF n=11 thoraces), *period* mutants did not have decreased polyubiquitin, or p62/ref(2)P aggregate accumulation in response to iTRF (*ad lib* n=10, iTRF n=10 thoraces); scale bar=50 μm. (See Methods and SI for trials, statistics, and source data; n=number of flies unless otherwise indicated; n.s.=p>0.05, *=p<0.05, **=p<0.01, ***=p<0.001, ****=p<0.0001; p-values were obtained by ANOVA followed by Tukey's post-hoc test (**a**, **g**–**i**) and log-rank analysis (**b**, **c**, **f**). Center values=averages; error bars=SEM.).

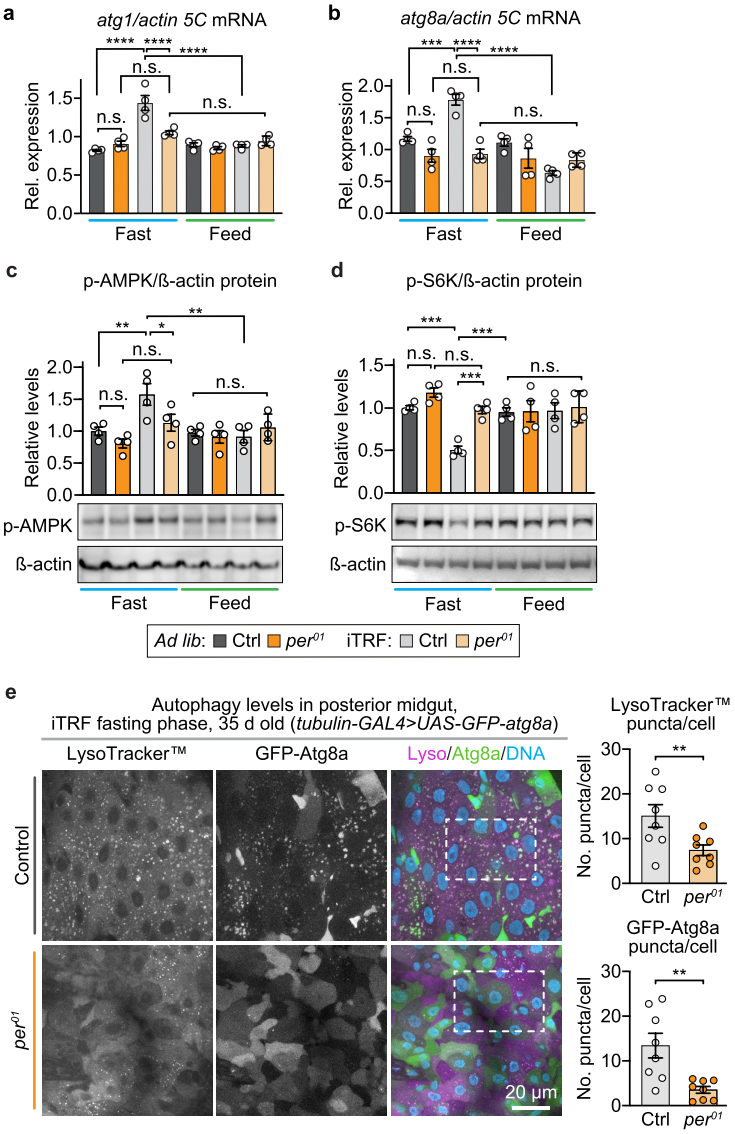

Extended Data Fig. 5 | *period* mutants are defective in autophagy regulation and autophagy induction in response to fasting. a, **b**, Similar to circadian genes, iTRF increased the peak amplitude of (**a**) *atg1* and (**b**) *atg8a* mRNA expression during the fasting period in wild-type flies (gray) but not *period*^{01} mutants (orange) (each dot=1 sample of 30 flies; each bar=average of 4 biological repeats). **c**, **d**, *period*^{01} mutants (orange) had (**c**) reduced activation of AMPK and (**d**) high levels of TORC1 activity as marked by S6K phosphorylation, both in response to fasting during iTRF, compared to controls (gray) (each dot=1 sample of 30 flies; each bar=average of 4 biological repeats); see also Extended Data Fig. 10. **e**, Representative images of posterior midgut cells during fasting phase of iTRF of 35-day-old flies labeled with LysoTracker™ (magenta), GFP-Atg8a (green), and DAPI to label the DNA (blue), showed that control animals (n=8 guts; each dot represents 2-3 Z-stacks of the posterior midgut of 1 animal) had high levels of LysoTracker™ and GFP-Atg8a puncta compared to *period* mutants (n=8 guts); scale bar=20 µm; white dashed boxes on images represent inset area presented in Fig. 3g. (See Methods and SI for trials, statistics, and source data; n=number of flies unless otherwise indicated; n.s.=p>0.05, *=p<0.05, **=p<0.01, ***=p<0.001, ****=p<0.0001; p-values were obtained by ANOVA followed by Tukey's post-hoc test (a-d) and unpaired, two-tailed t-test (**e**). Center values=averages; error bars=SEM.).

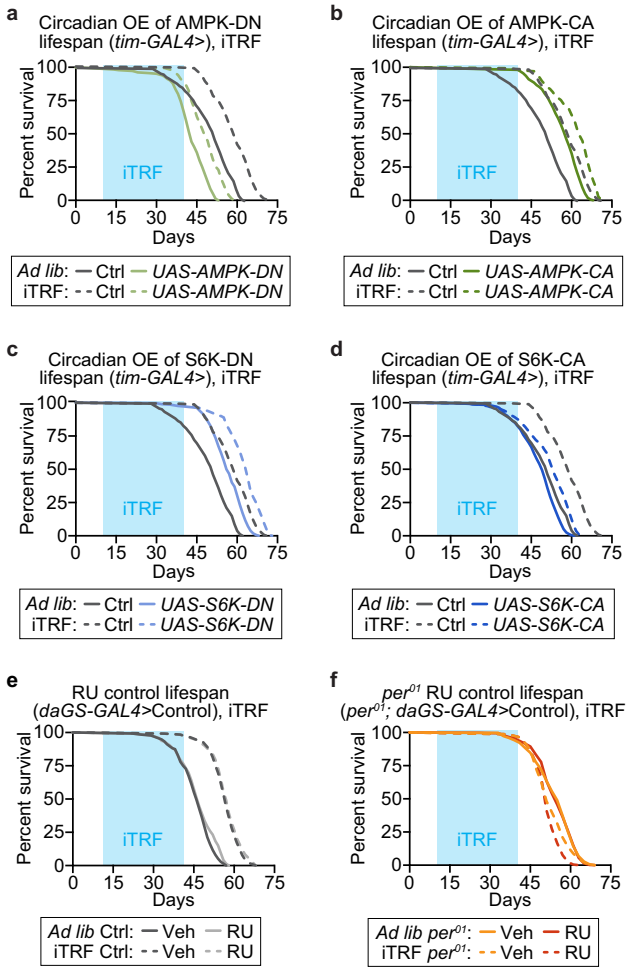

Extended Data Fig. 6 | Circadian manipulation of upstream metabolic and autophagy regulators partially determines lifespan response to iTRF. Light blue boxes on graphs indicate duration of iTRF during lifespan. **a**–**d**, Relative to controls (gray: ad lib, solid, n=161; iTRF, dashed, n=164), which had an ~20% increase in mean lifespan in response to iTRF, circadian overexpression of: (**a**) dominant-negative (DN) AMPK (K57A, sage green) shortened the lifespan of animals on *ad lib* diets (solid, n=184) and caused a 13% increase in mean lifespan in response to iTRF (dashed, n=170); (**b**) constitutively active (CA) AMPK (T184D, dark green) extended lifespan on *ad lib* diet (solid, n=156) and caused an 8% increase in mean lifespan in response to iTRF (dashed, n=134); (**c**) dominant-negative (DN) S6K (KQ, light blue) extended lifespan on *ad lib* diet (solid, n=292) and caused a 12% increase in mean lifespan in response to iTRF (dashed, n=180); (**d**) constitutively active CA-S6K (STDETE, medium blue) minimally shortened lifespan on *ad lib* diets (solid, n=237) and caused an 8% increase in mean lifespan in response to iTRF (dashed, n=282). **e**, **f**, RU486 feeding did not influence control (**e**) or per^{01} (**f**) lifespan in flies lacking UAS transgenes (control: *ad lib* n=136-146, iTRF n=129-142; per^{01}: *ad lib* n=294-501, iTRF n=238-415). (See Methods and SI for trials, statistics, and source data; n=number of flies; p-values were obtained by log-rank analysis (**a**–**f**)).

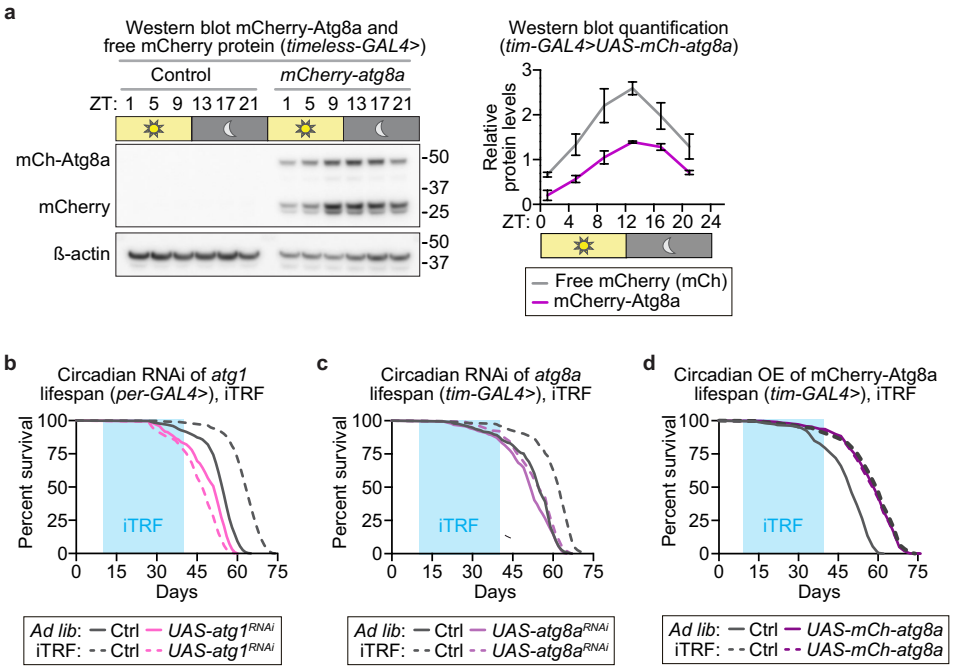

Extended Data Fig. 7 | Circadian regulation of Atg8a is necessary for iTRF and sufficient to extend lifespan. a, Using *tim*-GAL4 to drive expression of *mCherry-atg8a*, we confirmed oscillating mCherry-Atg8a and free mCherry protein expression by western blot analysis (see also Supplementary Fig. 1), which demonstrated circadian autophagic flux in controls on *ad lib* diet (each lane=30 flies; each time point of quantification=average of 3 biological repeats). **b**–**d**, Solid lines represent ad lib flies; dashed lines represent iTRF flies; light blue boxes on graphs indicate duration of iTRF during lifespan. RNAi-mediated circadian knockdown of (**b**) *atg1* (pink: *ad lib* n=217, iTRF n=166) and (**c**) *atg8a* (purple: *ad lib* n=196, iTRF n=139) was necessary for iTRF-mediated lifespan extension (controls, gray: *ad lib* n=194-316, iTRF n=196-409. (**d**) Circadian overexpression of mCherry-Atg8a was sufficient to extend lifespan on *ad lib* diet (solid lines: gray, control n=185; purple, mCh-atg8a n=422) and responded minimally to iTRF (dashed lines: gray, control n=421, purple, mCh-atg8a n=437). (See Methods and SI for trials, statistics, and source data; n=number of flies unless otherwise indicated; p-values were obtained by log-rank analysis (**b**–**d**). Center values=averages; error bars=SEM.).

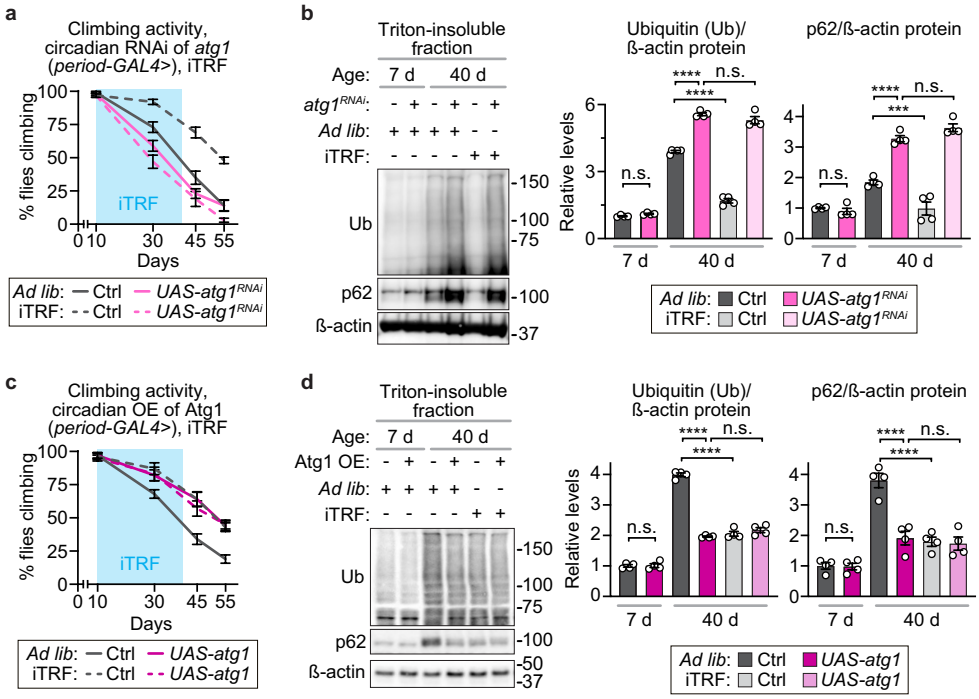

Extended Data Fig. 8 | *atg1* is necessary and sufficient for iTRF-mediated delays in aging-associated climbing defects and protein aggregation. **a**, **c**, Light blue boxes on graphs indicate duration of iTRF during lifespan. **a**, **b**, Relative to controls (gray), circadian knockdown of *atg1* (pink) increased aging markers of (**a**) climbing defects (n=10 vials of 10 flies/condition/genotype/timepoint) and (**b**) protein aggregation (each lane=30 flies; each time point of quantification=average of 4 biological repeats) and made flies resistant to the effects of iTRF (dashed lines, lighter shades), relative to *ad lib* diets (solid lines, darker shades). **c**, **d**, In contrast, relative to controls (gray), circadian overexpression of *atg1* (magenta) decreased aging markers of (**c**) climbing defects (n=10 vials of 10 flies/condition/genotype/timepoint) and (**d**) protein aggregation (each lane=30 flies; each time point of quantification=average of 4 biological repeats; see also Supplementary Fig. 1) and also made flies resistant to the effects of iTRF (dashed lines), relative to *ad lib* diets (solid lines). (See Methods and SI for trials, statistics, and source data; n=number of flies unless otherwise indicated; n.s.=p>0.05, ***=p<0.001, ****=p<0.0001; p-values were obtained by ANOVA followed by Tukey's post-hoc test (**a**–**d**). Center values=averages; error bars=SEM.).

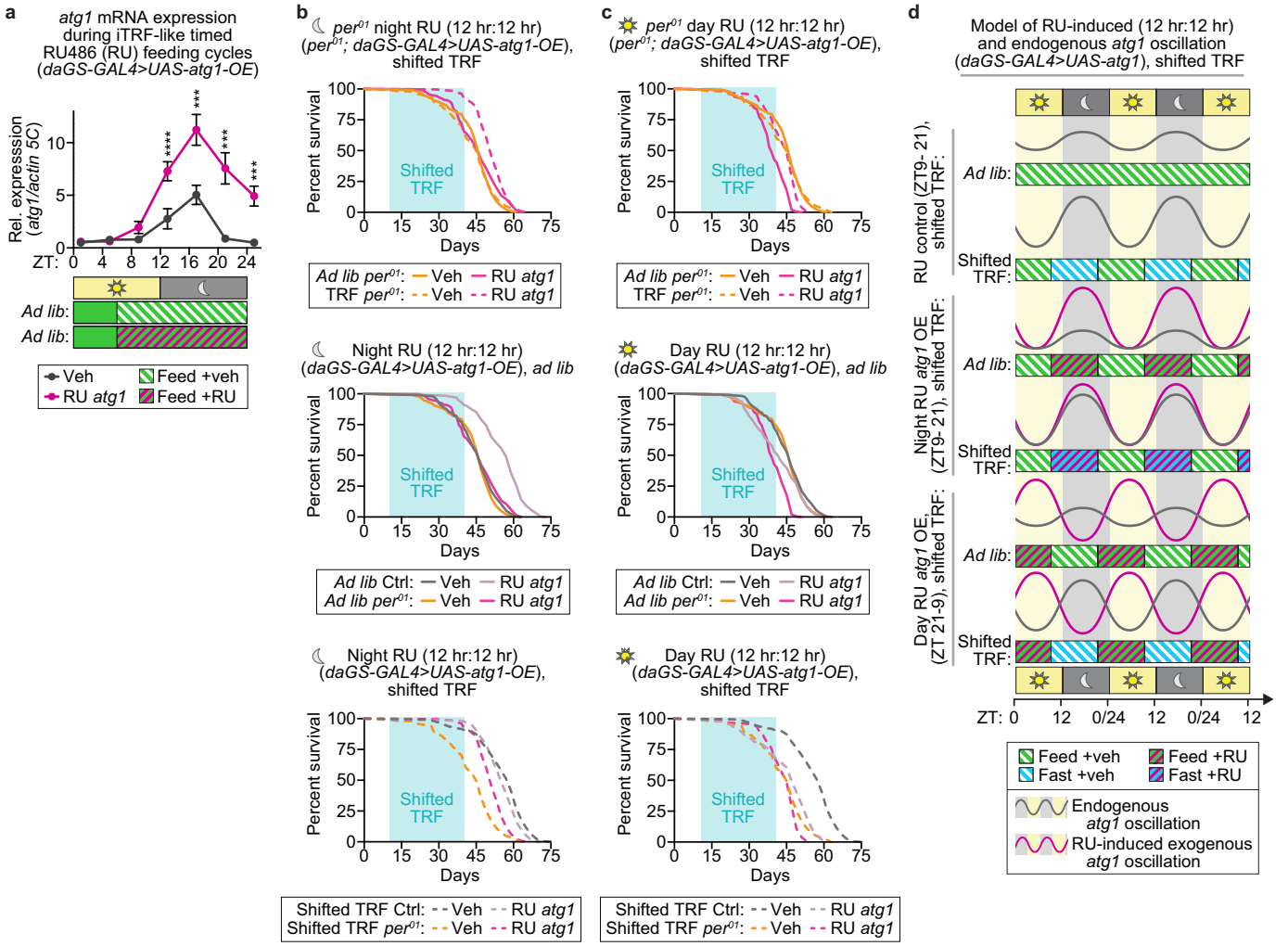

Extended Data Fig. 9 | Enhanced autophagy specifically during the night phase is necessary and sufficient for TRF-mediated lifespan extension. **a**, RU-induced overexpression of *atg1* during iTRF-like phases of the circadian cycle causes circadian enhanced, night-specific expression of *atg1* (n=4 biological replicates of 30 flies/timepoint/condition; unmarked=n.s.). **b**, **c**, Light aqua boxes on graphs indicate duration of shifted-TRF during lifespan. **b**, Relative to *ad lib* diet (*period*^{01} mutants *ad lib*, solid orange, n=225), neither night-biased 12:12 treatment of shifted TRF (dashed orange, n=228) or RU-induced *atg1* expression (solid magenta, n=319) alone extended the lifespan of *per*^{01} mutants. Combined, night-biased 12:12 shifted TRF and RU-induced *atg1* expression modestly increased lifespan of *per*^{01} mutants (dashed magenta, n=239). **c**, Replotted here are *per*^{01} mutants on *ad lib* diet (solid orange, n=225) and on night-biased 12:12 shifted TRF (dashed orange, n=228). Day-biased 12:12 RU-induced exogenous *atg1* expression decreased the lifespan of *per*^{01} mutants (solid magenta, n=206); this lifespan was increased by night-biased shifted TRF (dashed magenta, n=192). Also shown below are re-plots comparing control and *per*^{01} mutant backgrounds with night (**b**) and day (**c**) biased RU-induced *atg1* expression on *ad lib* diet (second row) or shifted TRF (third row). **d**, Graphic schematic illustrating endogenous rhythms of *atg1* expression (gray) and the predicted effects of RU treatment and 12:12 TRF, either night biased and day-biased, on exogenous *atg1* expression. (See Methods and SI for trials, statistics, and source data; n=number of flies unless otherwise indicated; n.s.=p>0.05, ***=p<0.001, ****=p<0.0001; p-values were obtained by ANOVA followed by Tukey's post-hoc test (**a**) and log-rank analysis (**b**, **c**). Center values=averages; error bars=SEM.).

nature portfolio

Corresponding author(s): Matt Ulgherait1 Adil M. Midoun, Scarlet J. Park, Jared Gatto, Samantha J. Tener, Julia Siewert, Naomi Klickstein, Julie C. Canman, William W. Ja Mimi Shirasu-Hiza

Last updated by author(s): 08/11/2021

Reporting Summary

Nature Portfolio wishes to improve the reproducibility of the work that we publish. This form provides structure for consistency and transparency in reporting. For further information on Nature Portfolio policies, see our Editorial Policies and the Editorial Policy Checklist.

Statistics

For all statistical analyses, confirm that the following items are present in the figure legend, table legend, main text, or Methods section.

n/a	Confirmed
☐	☒ The exact sample size (*n*) for each experimental group/condition, given as a discrete number and unit of measurement
☐	☒ A statement on whether measurements were taken from distinct samples or whether the same sample was measured repeatedly
☐	☒ The statistical test(s) used AND whether they are one- or two-sided *Only common tests should be described solely by name; describe more complex techniques in the Methods section.*
☐	☒ A description of all covariates tested
☐	☒ A description of any assumptions or corrections, such as tests of normality and adjustment for multiple comparisons
☐	☒ A full description of the statistical parameters including central tendency (e.g. means) or other basic estimates (e.g. regression coefficient) AND variation (e.g. standard deviation) or associated estimates of uncertainty (e.g. confidence intervals)
☐	☒ For null hypothesis testing, the test statistic (e.g. *F*, *t*, *r*) with confidence intervals, effect sizes, degrees of freedom and *P* value noted *Give P values as exact values whenever suitable.*
☒	☐ For Bayesian analysis, information on the choice of priors and Markov chain Monte Carlo settings
☒	☐ For hierarchical and complex designs, identification of the appropriate level for tests and full reporting of outcomes
☒	☐ Estimates of effect sizes (e.g. Cohen's *d*, Pearson's *r*), indicating how they were calculated

Our web collection on statistics for biologists contains articles on many of the points above.

Software and code

Policy information about availability of computer code

Data collection	Excel16.16.27 was used for data colection, Prism 7-8 was used for most statistical analysis, along with Fiji ImageJ version 2.0.0-rc-69/1.52p for image analysis.
Data analysis	Prism 7-8 was used for most statistical analysis, along with Fiji ImageJ version 2.0.0-rc-69/1.52p for image analysis.

For manuscripts utilizing custom algorithms or software that are central to the research but not yet described in published literature, software must be made available to editors and reviewers. We strongly encourage code deposition in a community repository (e.g. GitHub). See the Nature Portfolio guidelines for submitting code & software for further information.

Data

Policy information about availability of data

All manuscripts must include a data availability statement. This statement should provide the following information, where applicable:

- Accession codes, unique identifiers, or web links for publicly available datasets
- A description of any restrictions on data availability
- For clinical datasets or third party data, please ensure that the statement adheres to our policy

The authors declare that all data supporting the findings of this study are available, including replicate experiments, and will be made available upon reasonable request.

Field-specific reporting

Please select the one below that is the best fit for your research. If you are not sure, read the appropriate sections before making your selection.

☒ Life sciences ☐ Behavioural & social sciences ☐ Ecological, evolutionary & environmental sciences

For a reference copy of the document with all sections, see nature.com/documents/nr-reporting-summary-flat.pdf

Life sciences study design

All studies must disclose on these points even when the disclosure is negative.

Sample size	Power analysis was conducted for lifespans, usually 150 individual flies were used for statistical power.
Data exclusions	No data were excluded from results presented.
Replication	Prism7 (GraphPad) was used to perform the statistical analysis. Significance is expressed as p values (n.s.=p>0.05, *=p<0.05, **=p<0.01, ***=p<0.001, ****=p<0.0001). For two group comparisons unpaired, two-tailed t-test was used, when data met criteria for parametric analysis (normal distribution and similar variance). For more than two group's comparison ANOVA with Bonferroni, or Tukey's post-hoc test was performed. Kruskal–Wallis with Dunn's post-hoc analysis was used for non-parametric data. All plotted values represent means, with error bars representing SEM. All biochemical experiments were performed with a minimum of 4 biological replicates, repeated in 2-3 independent trials. For comparison of survival curves, log-rank (Mantel-Cox) analysis was used. For ad lib vs. iTRF (day 10-40) comparisons on 3% YE, control flies (w1118, Canton S) were tested 9 times, either as experimentals or as controls for other experiments (Fig 1b, 1d, 2d plus 2 repeats, 2f, ED 3j, ED 4c plus repeat, ED 4e). per01 mutants were tested 4 times (Fig. 2f, ED 4c plus repeat, ED 4e); per and tim CRISPR mutants were each tested twice (Fig. 2e plus repeat), clkJRK mutants were tested 3 times (Fig. 2d plus 2 repeats), and cyc01 mutants were tested 4 times (ED 4b plus 2 repeats, ED 4e). All other lifespans with genetic manipulations were tested 2 times, with the exception of large screens of alternative diets such as protein titrations (Fig. 1d, ED 4d-e), alternative TRFs (ED 1b-f), time windows for iTRF (ED2a-g), antibiotic treatment (ED 3i-j), or night vs day bias (Fig. 2f, Fig. 4h-i, ED 9b-c), as well as mCherry-Atg8 controls (ED 7d) and daGS driver controls (ED 6g-f), which were tested once. Titration of protein and lifespan with per01 mutants has been published previously.23 See SI Table 1 for details of all lifespan trials and SI Table 2 for raw source data.
Randomization	Initial lifespan screens were randomized and blinded. Follow up experiments were not randomized and blinded.
Blinding	Initial lifespan screen data were blinded and assigned number values and evaluated following all deaths over time.

Reporting for specific materials, systems and methods

We require information from authors about some types of materials, experimental systems and methods used in many studies. Here, indicate whether each material, system or method listed is relevant to your study. If you are not sure if a list item applies to your research, read the appropriate section before selecting a response.

Materials & experimental systems

n/a	Involved in the study
☐	☒ Antibodies
☒	☐ Eukaryotic cell lines
☒	☐ Palaeontology and archaeology
☐	☒ Animals and other organisms
☒	☐ Human research participants
☒	☐ Clinical data
☒	☐ Dual use research of concern

Methods

n/a	Involved in the study
☒	☐ ChIP-seq
☒	☐ Flow cytometry
☒	☐ MRI-based neuroimaging

Antibodies

Antibodies used	Membranes were probed with antibodies against AMPK phospho-T184 at 1:1000 dilution (Cell Signaling, 40H9); anti-phospho-S6K T398 (Cell Signaling, 9209), mCherry (Cell signaling, E5D8F), and horseradish peroxidase (HRP)-conjugated monoclonal mouse anti-actin antibody at 1:5000 dilution (Sigma-Aldrich, A3854). Rabbit antibodies were detected using HRP-conjugated anti-rabbit IgG antibodies at 1:2000 dilution (Cell Signaling, 7074). Mouse antibodies were detected using HRP-conjugated anti-mouse IgG antibodies at 1:2000 dilution (Cell Signaling, 7076). ECL chemiluminescence reagent (Pierce) was used to visualize horseradish peroxidase activity and detected by a CCD camera BioRad image station.
Validation	Validation available on manufacturer website.

Animals and other organisms

Policy information about studies involving animals; ARRIVE guidelines recommended for reporting animal research

Laboratory animals	w1118 Canton-S (CS) were used as a "wild-type" strain throughout this manuscript. UAS-DN-S6K (6911), UAS-CA-S6K (6914), UAS-DN-AMPK (32112), UAS-CA-AMPK (32110), UAS-atg1-RNAi (44034), UAS-atg8a-RNAi (34340), and UAS-atg1 (51654) were obtained from the Bloomington Stock Center and outcrossed to w1118 Canton-S (CS) for at least 10 generations. tubulin-GAL4 flies were obtained from John Carlson, UAS-mCh-atg8a and UAS-GFP-Atg8a from Eric Baehrecke, and daughterless-Gene-Switch (daGS) from David W. Walker; all were outcrossed to w1118 Canton-S (CS) for at least 10 generations. period (per01) mutants, timeless-GAL4, and period-GAL4 were obtained from Jaga Giebultowicz and, because they were last outcrossed many years ago, were outcrossed to w1118 Canton-S (CS) for 12 generations in the last 2 years. UAS-gRNA, UAS-CAS9 lines were those utilized in our previous papers and were outcrossed to w1118 Canton-S (CS) for five generations.22,39 Previously outcrossed cycle (cyc01) mutants were obtained from Sheyum Syed with a CS control strain. All experiments with multiple transgenes used flies that have undergone 12 generations of out-crossing into a w1118 Canton-S (CS) control and/or per01, w1118 Canton-S (CS) mutant background.
Wild animals	*Provide details on animals observed in or captured in the field; report species, sex and age where possible. Describe how animals were caught and transported and what happened to captive animals after the study (if killed, explain why and describe method; if released, say where and when) OR state that the study did not involve wild animals.*
Field-collected samples	*For laboratory work with field-collected samples, describe all relevant parameters such as housing, maintenance, temperature, photoperiod and end-of-experiment protocol OR state that the study did not involve samples collected from the field.*
Ethics oversight	*Identify the organization(s) that approved or provided guidance on the study protocol, OR state that no ethical approval or guidance was required and explain why not.*

Note that full information on the approval of the study protocol must also be provided in the manuscript.